The Minnesota Lectures on Extragalactic Neutral Hydrogen
ASP Conference Series, Vol. 106, 1996
Evan D. Skillman, ed.

HI Selection Effects and the Galaxy Mass Function

Stephen E. Schneider

Astronomy Program, University of Massachusetts, Amherst, MA 01003

Abstract. Many factors shape our view of the extragalactic universe. Chief among these are selection effects introduced by the sensitivity of astronomical instruments, competition with background noise and confusing sources of emission, and preconceptions about the nature of galaxies. In this chapter I examine selection effects from a general standpoint, mainly considering their influence on optical and HI observations, and conclude with presentation of results from a new Arecibo survey of a slice of the extragalactic sky at 21 cm. This new survey represents the most sensitive survey to date, covering about 50 square degrees at high Galactic latitudes, and uncovering a large population of previously uncataloged objects. I derive an HI luminosity function and conclude with an estimate of the total mass function of galaxies based on these data.

1. Introduction

A fundamental goal of extragalactic astronomy is to achieve a thorough census of the matter in the universe. With this knowledge we hope to address the great questions about the existence and nature of dark matter, the formation of large-scale structure, and perhaps the ultimate fate of the universe. Through observations of continuum and line emission over the entire electromagnetic spectrum, we attempt to track down the amount of that matter and its distribution in space. This is complex because the translation from observed emission to mass of material present often depends on unknown temperatures, densities, abundances, distributions, filling factors, etc., but usually astrophysics allows some plausible assumptions that permit us to make reasonable estimates.

In 21-cm astronomy, the good news is that the physics of the line transition is independent of all of these complicating terms under almost all possible conditions, so that HI mass estimates are straightforwardly derived from 21-cm line observations (see Kulkarni & Heiles 1988). However, despite this, the 21-cm census is far from complete. As in all fields of extragalactic observation, we need to account for the *selection effects* that determine which objects enter our samples and which are detected. Unlike the 1948 U.S. presidential pollsters, we want to make sure we don't determine only the characteristics of "galaxies that we can phone up" and declare that President Dewey has been elected! This brings us to the bad news: extragalactic 21-cm astronomy is probably more limited than any other field by subtle and insidious selection effects.

The problem is that extragalactic 21-cm-line astronomy is almost entirely dependent on observations at other wavelengths to define its domain. For the

most part observations are made of objects that have been first identified by their starlight, so any conclusions we try to draw about the HI properties of galaxies have optical selection effects folded in with the HI selection effects. Lately younger fields, like far-infrared astronomy, have provided new source lists for 21-cm observers, but this just adds a different layer of complication. I will briefly review the general emission properties of galaxies in section 2, pointing out that almost every other source of electromagnetic emission is intimately tied to stars and stellar nucleosynthesis. This is another reason why correcting the selection effects in 21 cm line studies is so important to pursue. The 21 cm line provides us with one of the only unique probes of the population of galaxies: the low excitation temperature of the line does not require stars to excite it, and since hydrogen is primordial, none of the processes of stellar nucleosynthesis are necessary for its presence.

One of the discoveries from optically-inspired 21-cm studies is that *within* individual galaxies the hydrogen frequently extends out to radii where little or no starlight is visible. It appears that star formation in the dense stellar regions has consumed most of the hydrogen. We might speculate whether there could be entire galaxies more comparable to the extended disk material, containing little starlight, but perhaps representing a significant portion of the extragalactic population. In such a scenario, optical selection effects would likely exclude these objects from ever entering our samples.

Just such large, low optical luminosity objects have in fact been encountered by a number of 21 cm observers. These discoveries have occurred mostly by accident, but they hint at the possible presence of a population of objects hitherto ignored. For example, in a calibration "off" scan to observations of a galaxy, I found a 200 kpc diameter HI structure in the Leo region outside the Virgo cluster (see Schneider 1989). This ring of gas contains $\sim 2 \times 10^9 M_\odot$ of HI, yet it has no detectable optical emission. It seems startling that an object with an angular size twice that of the Full Moon could remain unnoticed but for the accidental placement of a telescope during a calibration sequence. Likewise, Giovanelli & Haynes (1989) found a similarly large HI cloud surrounding a dwarf galaxy (McMahon et al. 1990) in one of their "off" scans.

Another surprise at 21 cm has been objects like "Malin 1," a huge disk galaxy found during a survey of low surface brightness dwarf galaxies in the Virgo Cluster (Bothun et al. 1987). Although this object looked like a dwarf, it proved to be at almost 20 times farther away, with a mass of HI $> 10^{11} M_\odot$! Further studies of objects classified as "dwarfs" have demonstrated that many are instead distant, large low surface brightness objects (Schneider et al. 1990, 1992).

These objects are individually fascinating, but it is unclear whether they are rare freaks or representatives of a large hidden population. To establish how common the HI-rich, optically-poor objects are we need to fully understand the selection effects on our observations and the procedures by which they can be corrected.

We will examine some basic ideas about luminosity functions in section 3, and how selection criteria interact with them to produce our samples of extragalactic objects in section 4. While these ideas are quite general for all wavelengths, HI surveys have some unique characteristics that we will focus on in

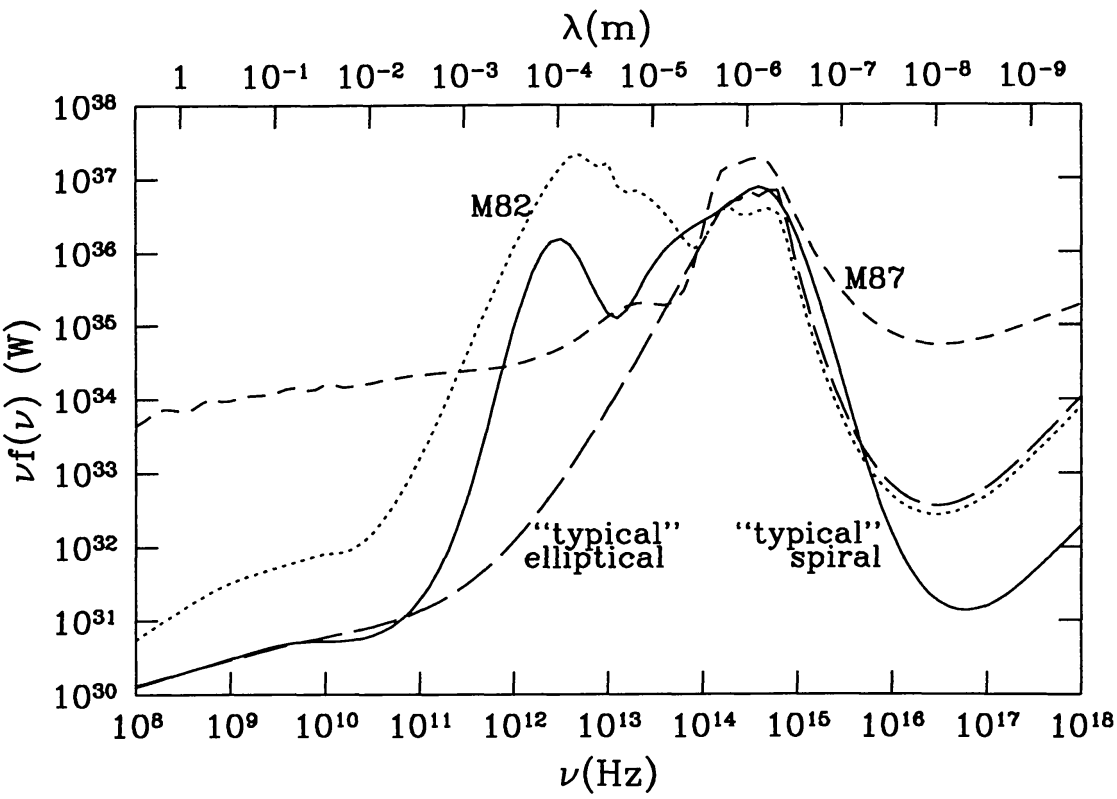

Figure 1. The power output from galaxies as a function of frequency. The top axis is labeled with the corresponding wavelength.

section 5. We conclude by presenting preliminary results from one of the largest independent HI surveys yet carried out.

2. The Galactic Spectrum

We are just entering the era of panchromatic studies of galaxies. While there are still large gaps for individual galaxies, through a wide range of new receiver technologies and space-based observations, we have now made measurements of galaxies from radio waves to gamma rays.

I illustrate the total continuum power output over ten orders of magnitude of frequency for a range of galaxy types in Figure 1. The figure shows a log-log plot of νf_ν against frequency. The results for "typical" elliptical and spiral galaxies are based on measurements of several objects spanning different wavelengths. Unusual galaxies like M87 and M82 tend to be better observed, but I caution that the data are particularly sparse in the ultraviolet through soft x-ray portions of the spectrum as well as the millimeter and submillimeter wavelengths, so some uncertain extrapolations have been used.

Recall that the total power output is $\int f_\nu d\nu = \int \nu f_\nu d(log\nu)$. Thus the relative power output in any feature can be "eyeballed" from the figure by multiplying its log-width $\Delta(log\nu)$ times its height νf_ν. This shows that spirals and irregulars like M82 produce comparable amounts of power in the submillimeter to far-infrared portion of the spectrum as in the optical.

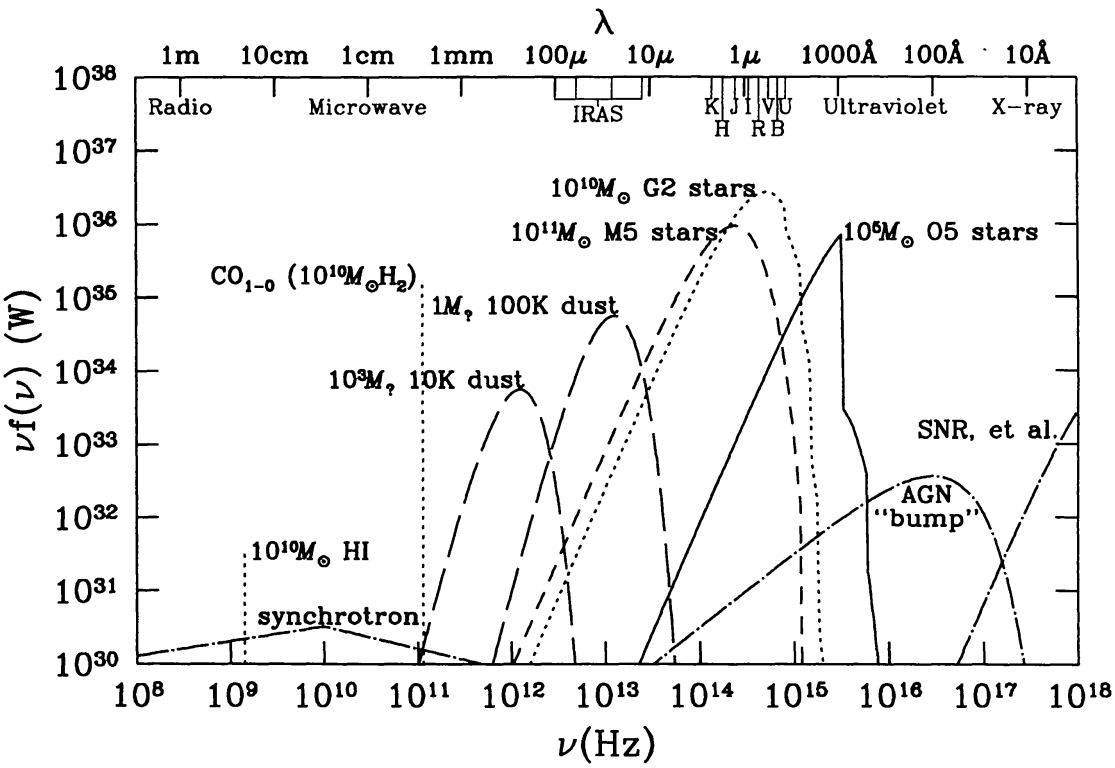

Figure 2. Power output from several sources of galactic emission. Most of the curves are labeled according to the solar masses of material producing the emission. The dust emission depends in such a complex way on the grain sizes and compositions that only relative masses (labeled in terms of $M_?$) are shown for two temperatures. Sources of non-thermal emission are shown unscaled just to indicate their relative shapes. Various of the wavebands commonly observed are labeled along the top axis.

As a guide to interpreting these spectra, I display some possible components in Figure 2. For example, note how a small total mass of O-stars can produce as much power output as 10^5–10^6 times more matter in the form of solar-type or M-dwarf stars. Note that several orders of magnitude less mass in the form of red giant G or M stars would produce similar power outputs. The art of modeling the optical portion of the spectrum is to reproduce the shape of the optical portion of the spectrum with a plausible distribution of stellar types. Deriving an actual mass of stellar material is non-trivial since large masses of late type dwarfs can be added with little change in the total power output.

The large power output from spirals and irregulars in the submillimeter and far-infrared appears to be explained by dust. This is really just reprocessed starlight. The mass of dust producing this major component of the power output is not easy to determine, depending as it does on the size and composition of the dust grains. Note also how a large mass of very cold dust (like the M stars) can be hidden within the total emission. Actually, the mass of dust is not itself believed to be a very significant fraction of the total mass of a galaxy.

However the dust is likely associated with molecular clouds that may represent a significant component of the galaxies.

Radio and x-ray emission from galaxies is generally a relatively small fraction of the total power output. It is likely produced by thermal (free-free) emission from HII regions and synchrotron emission from supernova remnants. There may also be components associated with active galactic nuclei. These forms of emission are in various ways connected with stars, star formation, and star death, and are basically correlated with stellar content, except in galaxies like M87 where an AGN and associated jets may produce an exceptionally large non-thermal output.

Even most line emission is closely tied to stars and star formation. Many lines are observed, and each is an important probe of a galaxy's interstellar medium (or outer atmospheres of stars), but these spectral lines ultimately rely on the power produced by starlight to put the atoms in the upper level of the transition. One example shown in Figure 2 is the CO_{1-0} line. Like the dust, CO is a surrogate tracer for the major mass component of molecular clouds H_2. It is a strong line, but it is also difficult to interpret since it depends on the temperature, density, and clumpiness of the gas, and consequently on the relative location of the gas and the stars that power the transition (see, for example, Puget 1989, Stein & Soifer 1983, Telesco 1988). To further complicate matters, in other galaxies—especially those that have undergone little star formation—the enrichment of the interstellar gas in heavy elements may differ.

Last of all, note the 21 cm transition in Figure 2. The strength shown here is for a typical Doppler-broadened line width, which is invisibly narrow on this graph. Although the integrated power involved is small, the line is the simplest tracer of this major component of galaxies' composition. What makes the 21-cm line so simple to interpret is that its excitation temperature is only a fraction of a degree Kelvin. The intergalactic background x-ray radiation can keep the line thermalized (Deguchi & Watson 1985), so it is almost always found with the same ("geometric") fraction of atoms in the upper level of the hyperfine transition, and collisions do not alter that ratio. Therefore the emission in the line is directly proportional to the number of atomic hydrogen atoms, regardless of their temperature or density. Since starlight is not necessary to power the 21 cm line, and since hydrogen is a primordial element, the 21 cm line measures something completely independent of stars.

3. Luminosity Functions

To address the question of how much mass different galaxies contribute to the total, we begin by examining their luminosities, which are more directly observable. The emission from a set of galaxies in a particular waveband or in a spectral line can be characterized by a luminosity function Φ. This is a distribution function (essentially a histogram) of the number of galaxies in each range of luminosity. Luminosity functions have some generally common characteristics that we will examine in this section, and we will begin to look at how a luminosity function is translated into a mass function—which is our ultimate goal.

The function Φ is often written as a density so that integrating over all luminosities $\int \Phi(L)dL$ gives the total number of galaxies per some volume unit like 1 Mpc^3. Since ΦdL gives the total number of galaxies of each luminosity, it can be multiplied by other galaxy properties and integrated to derive population totals (or totals within narrower luminosity ranges) for other properties. For example, the total luminosity of a population is:

$$L_{tot} = \int_0^\infty L\Phi(L)dL \; . \tag{1}$$

In principle, if we know the relationship between mass and luminosity we can integrate

$$M_{tot} = \int_0^\infty M(L)\Phi(L)dL \tag{2}$$

to determine the total mass. This however assumes some simple relationship between mass and luminosity, which may not be realistic as we shall discuss further below.

Classically, Φ is determined in a well-studied region where the galaxy distances are known and deep integrations have generated quite complete samples. This has usually confined such studies to nearby galaxy clusters, which is a point to keep in mind in case there are biases in the galaxy properties in such high density regions.

One of the features of galaxy luminosity functions that appears to be true at most wavelengths is that the number counts grow larger at fainter luminosities like the luminosity to some negative power. This power law behavior, $\Phi(L) \propto L^\alpha$ where $\alpha < 0$, is a common sort of distribution in nature, describing the size distribution of asteroids and turbulence for example.

The power law behavior of Φ appears to persist over several orders of magnitude in galaxy luminosity. At very high luminosities the number counts of galaxies drop off much more rapidly than the power law, and at very low luminosities the definition of a galaxy must break down as the luminosity approaches the range of globular clusters. The faint end is not very well observed though, so this low-luminosity turnover or cutoff has not been characterized.

One frequently employed description of the luminosity function is that developed by Schechter (1976). The Schechter function is a power law with an exponential drop-off at high luminosities:

$$\Phi(L) \propto (L/L_\star)^\alpha e^{-L/L_\star} \tag{3}$$

This function is plotted in Figure 3. The value $L_\star$ characterizes the highest luminosities before the number counts start to drop off significantly from the power law distribution. $L_\star$ is the luminosity of the most common type of bright galaxy, which are therefore some of the better known, and is approximately the luminosity of the Milky Way and M31.

We can use the Schechter function to explore which galaxies contribute most to the total luminosity of galaxies. In Figure 3, the shape of the luminosity function is shown for values of the power law index α from -1 to -2. The shapes of these functions do not look very different, but the resultant fraction of the luminosity contributed by different decades of luminosity is quite different,

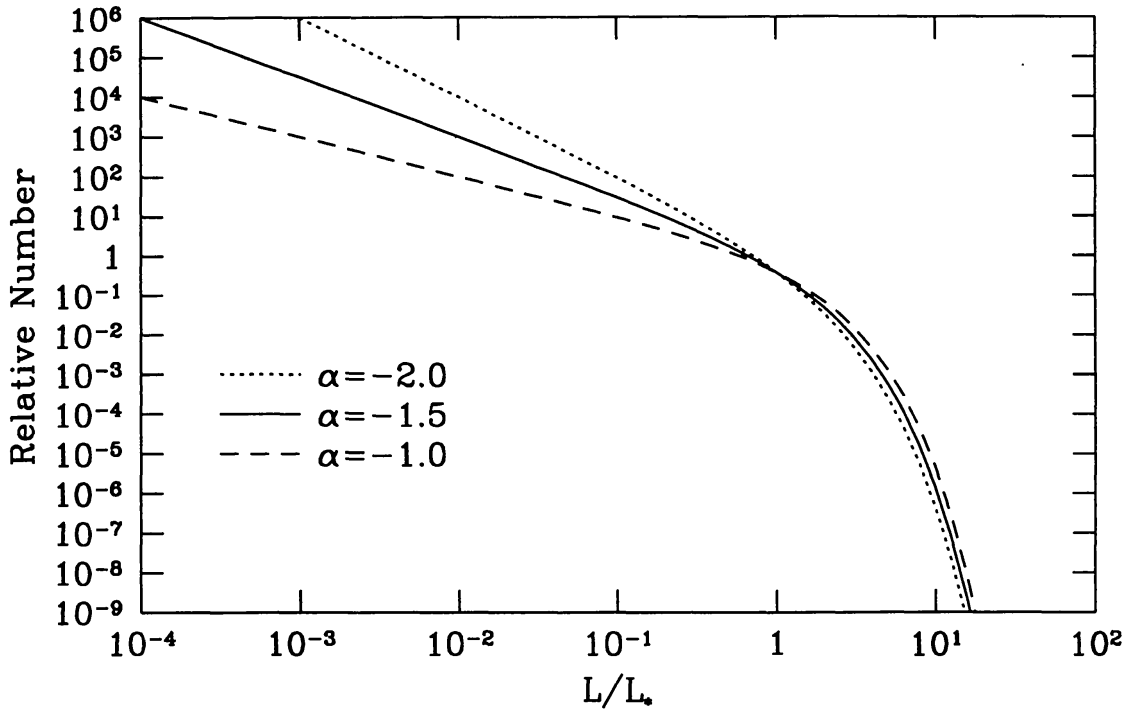

Figure 3. The distribution of galaxy luminosities or masses as modeled by the Schechter luminosity function assuming different power law indices.

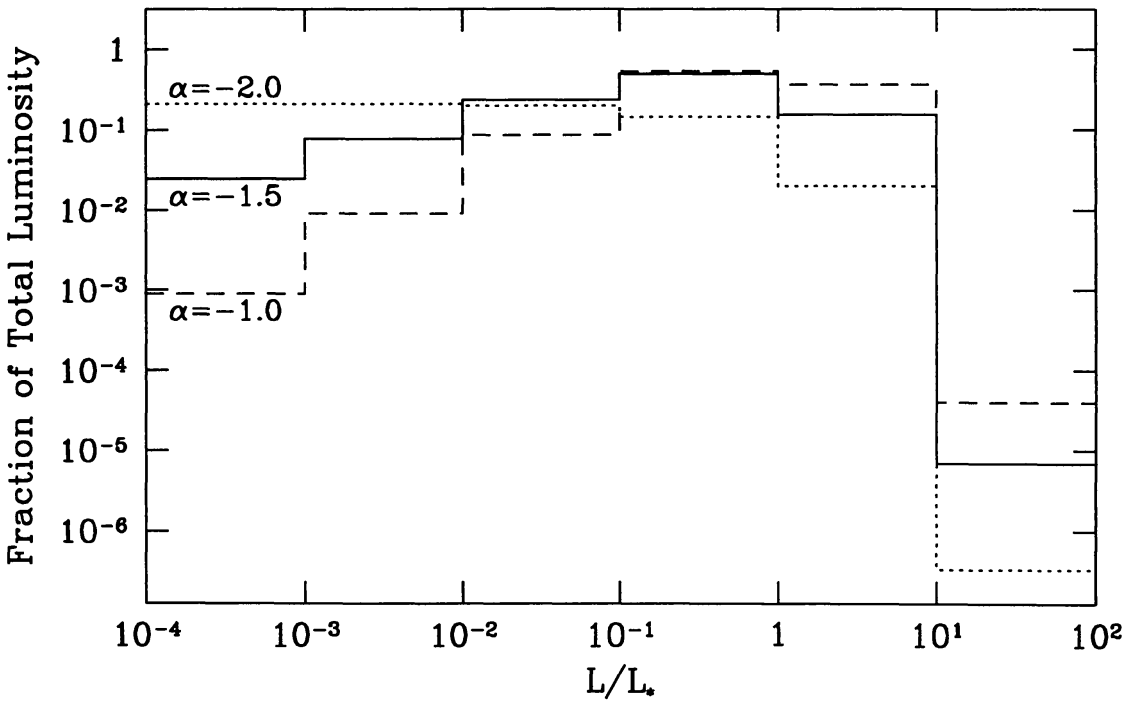

Figure 4. The total contribution to the luminosity function from different luminosity decades when assuming different power law indices in a Schechter luminosity function.

as shown in Figure 4. If the power law is shallower, the main contribution to the total luminosity is from galaxies with luminosities near $L_\star$. However, if the power law were as steep as -2, the lowest luminosity galaxies contribute the largest fraction of light.

Estimates of the Schechter function generally indicate $\alpha \sim -1.25$. The power law appears to be even shallower than this outside of clusters, perhaps because the dwarf galaxies corresponding to the cluster dwarf elliptical populations have not been well-cataloged. (See Binggeli, Sandage, & Tammann 1988 for a review of luminosity function determinations.) Such shallow power laws would indicate that there is no major luminosity contribution from faint objects.

However, the more important question is what this relationship signifies for the total *mass* of galaxies. For example, low luminosity galaxies may have a larger mass-to-light ratio than brighter galaxies since their interstellar mediums are more weakly confined by their gravity and are probably less efficient at forming stars. If it were possible to characterize the mass-to-light ratio as another power law, $M/L \propto L^\beta$, then the *mass* per luminosity interval would look like Figure 4 for a Schechter exponent of $\alpha' = \alpha + \beta$. (Note that this is not the same as the power law exponent in the *mass function*—the number per mass interval—which would have a distribution function obeying $\Phi(M)dM = \Phi(L)dL$.) If β is negative as I have argued, then α' would be closer to -2 than α, and low luminosity galaxies would be more significant contributors to the total mass than they are to the total luminosity.

4. Selection Effects

While it is interesting to speculate that faint galaxies, like M stars, may be the major contributor to the total galaxian mass, the possibility is (at best) only weakly suggested by the evidence. However, the evidence is well known to have biases against faint galaxies. Large corrections are necessary to account for these selection effects, and there are large uncertainties in these corrections.

Like dim stars, dwarf galaxies are detectable only to relatively small distances in a flux-limited survey. This can be corrected by adjusting the results according to the volume of space effectively surveyed. Galaxy detections are also limited by the galaxy's surface brightness relative to the "background" noise, which is less easily corrected. Finally, galaxies must also be identified by their morphology, which is primarily a minimum-size requirement, but this may also include subtler effects that are difficult to quantify.

To correct for the effects of these selection criteria, we use simple models of the data and our detection methods. The methods for making these corrections are similar whether we are examining optical or 21 cm data, but the kind of galaxies most affected are often quite different as we shall explore below.

4.1. Flux Limits

Flux limits have a surprising effect when they interact with the galaxy luminosity function. The combination of a flux limit with the turnover in the luminosity function results in a preferred distance at which galaxies are detected. This can be shown by integrating the Schechter luminosity function over the range of luminosities detectable at distance d and multiplying by the volume $d^2 \Delta d\Omega/3$

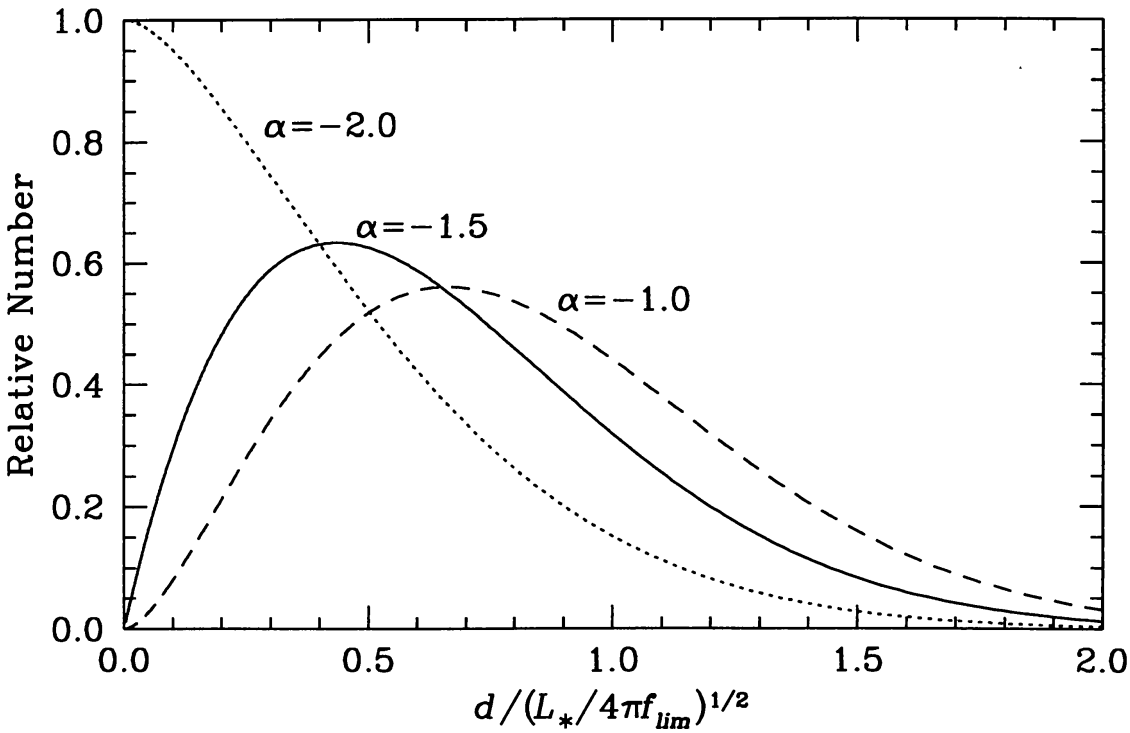

Figure 5. The distance distribution of a flux-limited sample of galaxies obeying a Schechter function with various power law indices. The distances are scaled to the distance at which an $L_\star$ galaxy reaches the flux limit, and the distributions are scaled to give the same total number of galaxies detected out to the flux limit f_{lim}.

at that distance:

$$N = d^2 \Delta d \frac{\Omega}{3} \int_{4\pi d^2 f_{lim}}^{\infty} (L/L_\star)^\alpha e^{-L/L_\star} dL \tag{4}$$

where f_{lim} is the limiting flux. The result of this integration is shown in Figure 5. The greatest number of galaxies is detected at about half the distance at which an $L_\star$ galaxy drops to the flux limit. This behavior results from the competition between the increasing volume of space, which dominates when $d \ll \sqrt{L_\star/4\pi f_{lim}}$, while at large distances the exponential cutoff at high luminosities causes a rapid decrease in galaxy counts.

Thanks to this effect, various galaxy surveys pick out large scale structures at different distances. Since $L_\star$ corresponds to an absolute magnitude of about -20, Dreyer's (1888) *New General Catalogue (NGC)*, with a limiting magnitude of about 14, picks out galaxies at about half as far as the distance modulus of 34, or about 30 Mpc. Therefore structures like the Virgo Cluster and "Local Supercluster" stand out. Zwicky's (1962–8) *Catalogue of Galaxies and Clusters of Galaxies (CGCG)* pushes down to a limiting magnitude of about 15.5, so that structures about two times more distant, like the Pisces-Perseus supercluster, become prominent as shown in Figure 6 (also see Giovanelli & Haynes 1988).

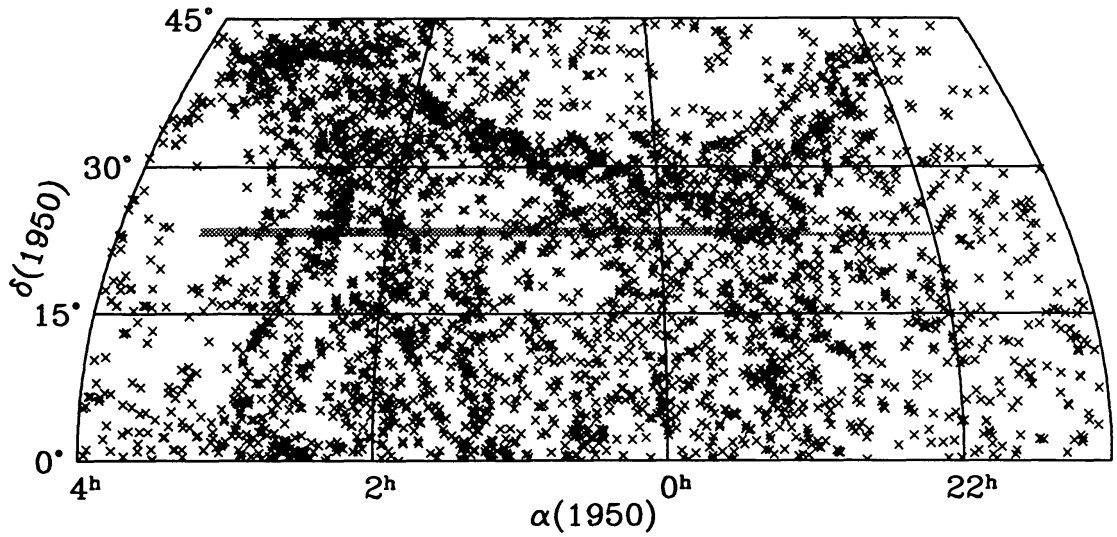

Figure 6. Sky map of galaxy positions in the general direction of the Pisces-Perseus supercluster. Because the limiting magnitude is about 15.5, structures at a redshift of about 5000 km s^{-1} are most evident. The gray region was surveyed at 21 cm as is discussed later in this chapter.

HI observations are also affected by flux limits of course. For a given limiting sensitivity the distance out to which a mass of HI, M_{HI} can be detected is:

$$d_{lim} = 65\mathrm{Mpc} \left(\frac{M_{HI}}{10^9 M_\odot} \right)^{0.5} \left(\frac{\int S_{HI} dv}{1\mathrm{Jy\ km\ s^{-1}}} \right)^{-0.5} \tag{5}$$

where $\int S_{HI} dv$ is the minimum integrated line strength that can be measured.

We will see later that the distribution of galaxies' HI masses can be approximated by a Schechter function, so similar flux-limit effects apply. The "turnover mass" (the equivalent of $L_\star$) in the HI mass function is $M_{HI\star} \approx 10^{10} M_\odot$. Therefore with a sensitivity limit of 1 Jy km s^{-1}, a sample of randomly-selected galaxies would most commonly be detected at distances less than 100 Mpc (or about 7500 km s^{-1}). This was a fairly typical detection limit at the former Green Bank 300 ft telescope. In surveys made with low-temperature receiver systems at Arecibo the typical flux limit was about four times lower, corresponding to distances about two times larger.

This flux-limit effect is easy to overlook because HI observations are usually made of objects selected on the basis of their optical emission. With information about the galaxy's visual appearance the 21 cm integration time is often tailored to expectations about the amount of HI. In addition, emission at the two wavelengths may be inherently correlated—larger galaxies generally have more stars and more HI—so that a sample with a visual flux limit will also have a related HI flux limit. Thus HI observations based on an optically-selected sample will tend to be biased toward the smaller of the distances favored by either of the flux limits.

It is important to recognize that using a visually flux-limited sample of galaxies has a second more insidious effect. The resulting observations may appear to indicate that the visual and HI emission are more correlated than they actually are because the high HI/low visual luminosity objects will tend to be excluded. While high visual/low HI galaxies (S0's, ellipticals) are well known, the converse may have been overlooked.

4.2. Surface Brightness Limits

Surface brightness limits also apply in both the optical and radio domains. Basically, the emission per unit area from galaxies is comparable to competing sources making it difficult to distinguish real sources from background variations. At visual wavelengths the receiver technology has improved to the point where the night sky brightness and even the surface brightness of emission from our own Galaxy make detection difficult. At 21 cm internal receiver noise is still the primary limiting factor. These effects are not easily quantified, but there is a growing recognition in the optical domain that there is a potentially large problem.

The blue luminosities and diameters of galaxies in the *Third Reference Catalog* (RC3; de Vaucouleurs et al. 1991) are plotted in Figure 7. Over a very wide range of luminosities the galaxies lie within a narrow locus of mean surface brightness around 24 mag arcsec^{-2} or about $10L_{\odot}$ pc^{-2}. Galaxies with surface brightnesses much higher (to the upper left) and much lower (to the lower right) are notably absent. This is quite surprising given the wide range of surface brightnesses observed inside of galaxies. After all, some outer disks of spiral galaxies have HI detected in regions where no optical emission is visible. Why then shouldn't there be dwarf galaxies with comparably low surface brightnesses?

The lack of fainter galaxies is partly an artifact of the way galaxy sizes are measured. Since diameters and fluxes are normally measured out to the 25 mag arcsec^{-2} isophote, the average surface brightness of a centrally brightened source has to be higher. Disney & Phillipps (1983) have shown further coincidences between observed galaxy surface brightness properties and the limiting surface brightnesses observed from Earth. Fainter surface brightnesses are now well within reach of modern detectors, but few systematic surveys have been completed and there are conflicting interpretations of the results (see McGaugh 1996).

For HI observations, there is little competition with background emission. Using single-dish radio telescopes, detection of surface densities of hydrogen down to $\sim 10^{19}$ cm^{-2} ($\sim 0.1M_{\odot}$ pc^{-2}) requires only relatively short integration times for most modern receiver systems. This is sufficient to detect most spiral galaxies well outside their optical disks. However, the "beam size" at 21 cm is often larger than the extent of the HI being observed so that "beam dilution" can limit the actual detectable surface brightness. With synthesis arrays the surface brightness sensitivity depends on other factors. Essentially the noise is equivalent to a single-dish telescope of the same total area, but the angular area is that of the "synthesized beam." Therefore, to reach the same surface brightness limit, longer integration times are necessary in proportion to the ratio

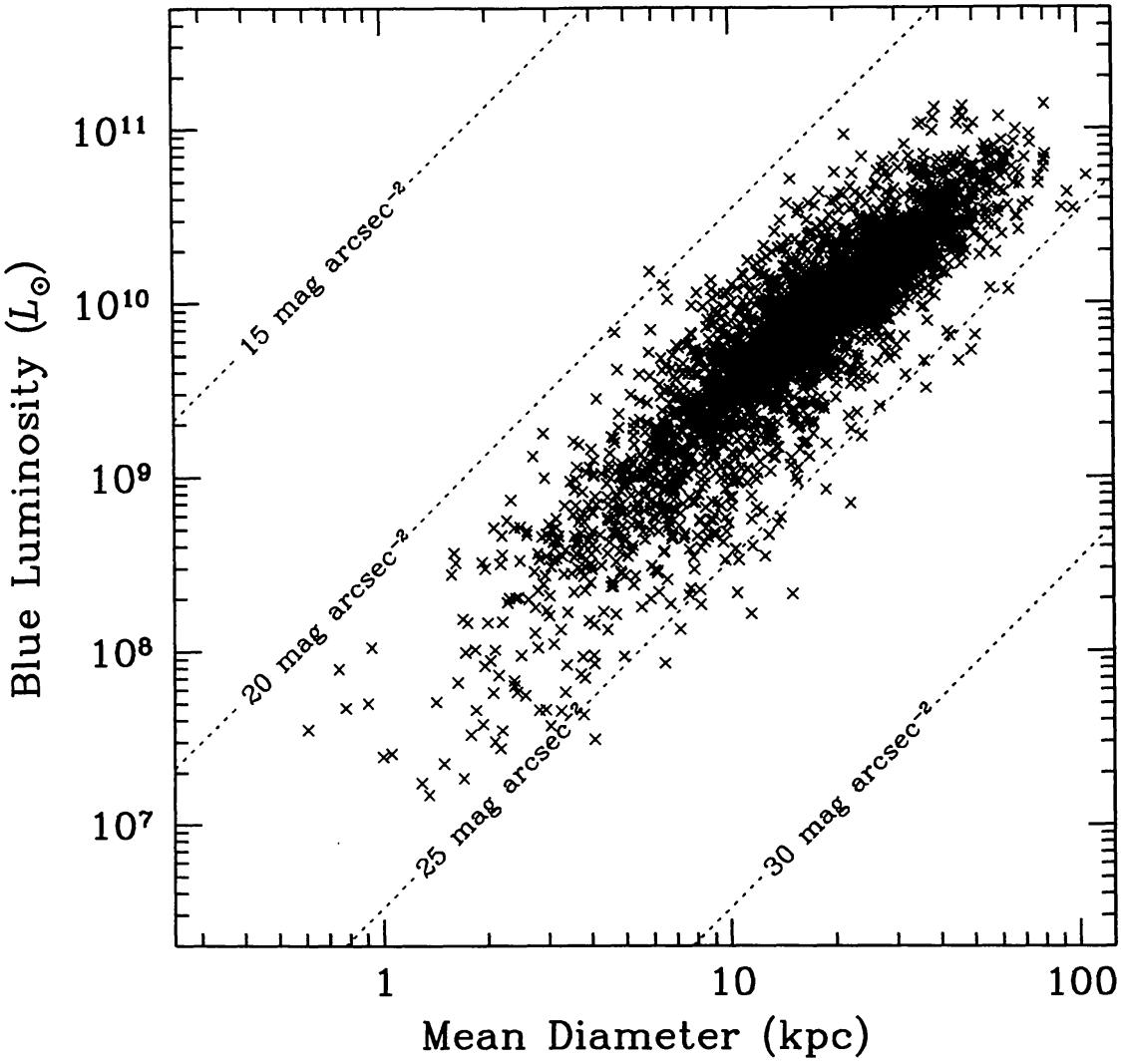

Figure 7. The diameters and luminosities of galaxies in the Third Reference Catalog. The diameters are the geometric mean of the major and minor axes measured at the 25 mag arcsec^{-2} isophote in blue or "photographic" wavebands. The luminosities are based on the total blue magnitudes. Both are based on distances determined from Galactocentric velocities and a value of the Hubble constant of $H_0 = 75$ km s^{-1} Mpc^{-1}.

of the area of the "primary beam" (of an individual array element) to the area of the synthesized beam.

At 21 cm there is an additional dimension to the surface brightness limits: the problem of detecting an HI signal in a one-dimensional spectrum. The HI signal profile has a width that depends on the mass of the object, the amount of circular rotation, and the inclination of the rotation to the line of sight. Wider profiles are more difficult to detect because they spread the signal over a wider frequency range, so the noise grows in proportion to $\sqrt{\Delta v}$. In an interesting twist, face-on galaxies have low optical surface brightness (the light is spread out over a larger solid angle), but they have higher "spectral" surface brightness since the signal is focused into a narrower Doppler-shift range.

In single-dish observations, the spectral surface brightness is usually the main consideration since beam dilution is essentially a flux-limit problem. In synthesis-array observations and large single-dish mapping programs, the data are often thought of as a cube with two spatial and one frequency axis. Spatial planes, or hybrid frequency/spatial planes are examined to uncover any sources of emission. In these data cubes, the practical unit of noise against which sources must be detected is the rms deviation in each beam and in each frequency channel. Detections are most enhanced when the beam size and channel width are closely matched to the source size since that maximizes the signal while minimizing the addition of noise from regions where no signal is present. However, as we will discuss later, it is usually necessary to sacrifice some surface-brightness sensitivity in order to identify the HI signal.

4.3. Galaxy Identification

The procedure by which galaxies are identified proves to be an extremely difficult selection effect to quantify. A concept of what a galaxy *should* look like has evolved in this century based on our growing experience with these objects. In its most general morphological sense, a galaxy might be defined as an extended source with a generally elliptical or circular profile. They are centrally brightened and fade fairly steadily to undetectably low surface brightnesses in their outermost regions.

Obviously a *physical* definition of galaxies would be preferable, perhaps something very general like "a distinct self-gravitating system with a mass $> 10^7 M_\odot$." The morphological definition implicitly assumes stars must be present, reaching a high surface density at the galaxy's center, but we have to be careful not to let our description of galaxies become a self-fulfilling prophecy. At the same time we want to avoid cluttering catalogs of galaxies with nearby Galactic nebulae.

There is no especially strong evidence that the major catalogs are badly incomplete, but there are troubling questions. Could the narrow range of observed surface brightnesses in Figure 7 be due in part to a predisposition toward galaxies with a particular appearance? Would a system that was not significantly brighter toward its center be dismissed as a Galactic HII region? Observations at new wavebands usually show much more overlap than difference with current optical catalogs, but since these observations are almost exclusively based on starlight or its surrogates, are they providing a good measure of completeness?

I fear that the problem will only get worse with modern cataloging systems. Computer identification schemes, including "neural nets" and "decision trees," are all rigorously based on preconceived notions of the morphology of galaxies, and they are often "exercised" or "trained" on sets of objects which agree with our current expectations for a galaxy. The huge numbers of objects that will soon spill forth from various digital surveys has the potential to illuminate, but it also has the potential to overwhelm.

To broaden the scope of our understanding of galaxies, what we need are more "blind" surveys, by which I mean surveys that are not based on the visual appearance of a galaxy or on emission at another wavelength that is highly correlated with the visual. One way is by identifying band-to-band differences that might signal a galaxy. For example, it is possible to use the IRAS survey's 60 to 100 μm emission to identify what are probably cool dust-bearing objects. In this way a source may be identified independent of its morphology, although perhaps not entirely independent of prior expectations about the construction of galaxies.

Another even more unbiased way to cast our nets is with spectral surveys. These can identify *any* object whose redshift places it outside of the Galaxy provided the emission line is excited, sufficiently strong, and the line is observable. Any of several spectral lines might be used, but HI is the most independent of optical emission for the reasons discussed earlier. HI has its own identification problems, of course, and these are discussed in the next section.

5. HI Surveys

To understand the selection effects in 21 cm HI astronomy, we will examine the observing procedures in detail. The spectral survey has some basic differences from optical surveys and some unique problems. For the most part, I will refer to single-dish observations in which a single spectrum in a single direction is observed at one time. This is changing somewhat as the field moves in the direction of synthesis array systems and multiple receivers, but the individual radio spectrum is still the basis of most 21 cm detections.

Radio observations are usually made with what is known as the "total power" or "on–off" method. In this method, illustrated in Figure 8, the position of a suspected HI source (the *on* position) is observed along with an identical observation in an empty (*off*) region. The total power detected at each frequency in the *off* scan is subtracted from the *on* scan to remove background emission, persistent interference, and instrumental response characteristics. The result, as shown in the figure, is a spectrum relatively free of features in which the HI signal of the galaxy stands out.

The sample spectrum in Figure 8 shows a few of the features frequently encountered. The galaxy appears to have a few mJy of radio continuum emission, which shows up as a broadband difference between the *on* and *off* spectra. In addition, there is a small amount of curvature in the *baseline* regions of the difference spectrum. This might be real, but it is more likely due to slight frequency response differences in the receivers between the two times and for the two total powers of the *on* and *off* positions. Baselines are commonly removed by subtracting a polynomial fit to regions outside of the frequency range where line

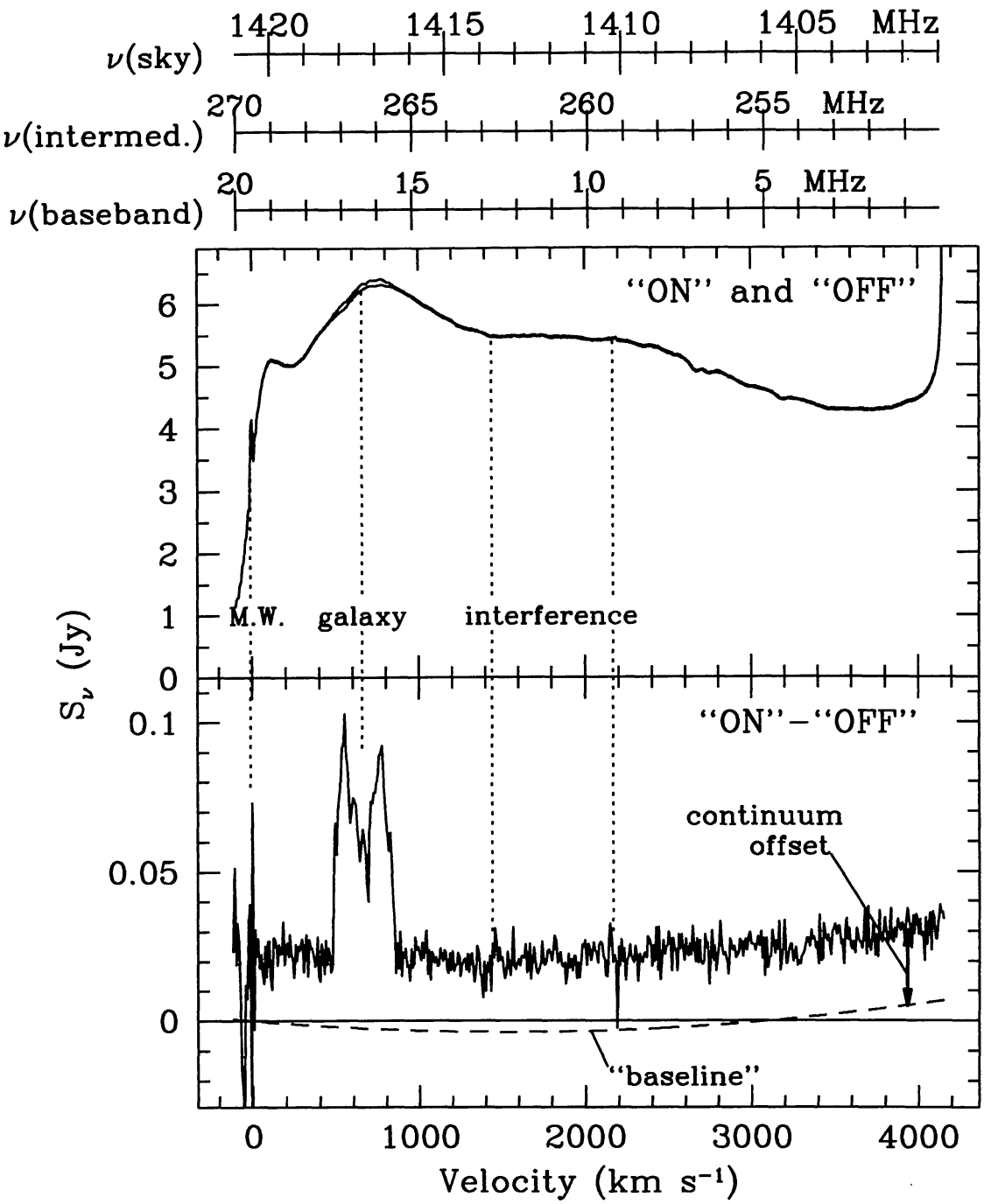

Figure 8. A basic *on–off* 21-cm spectrum. The upper panel shows the total power detected in each of two spectra at two positions on the sky, and the lower panel shows the difference spectrum. Both natural and man-made emission can enter into the spectrum at the frequency actually observed, or at one or more intermediate frequencies and the baseband frequency range used by the auto-correlation spectrometer as shown at the top of the figure. A second-order polynomial fit to the *on–off* baseline is also shown along with the slight offset between the total power at the two positions.

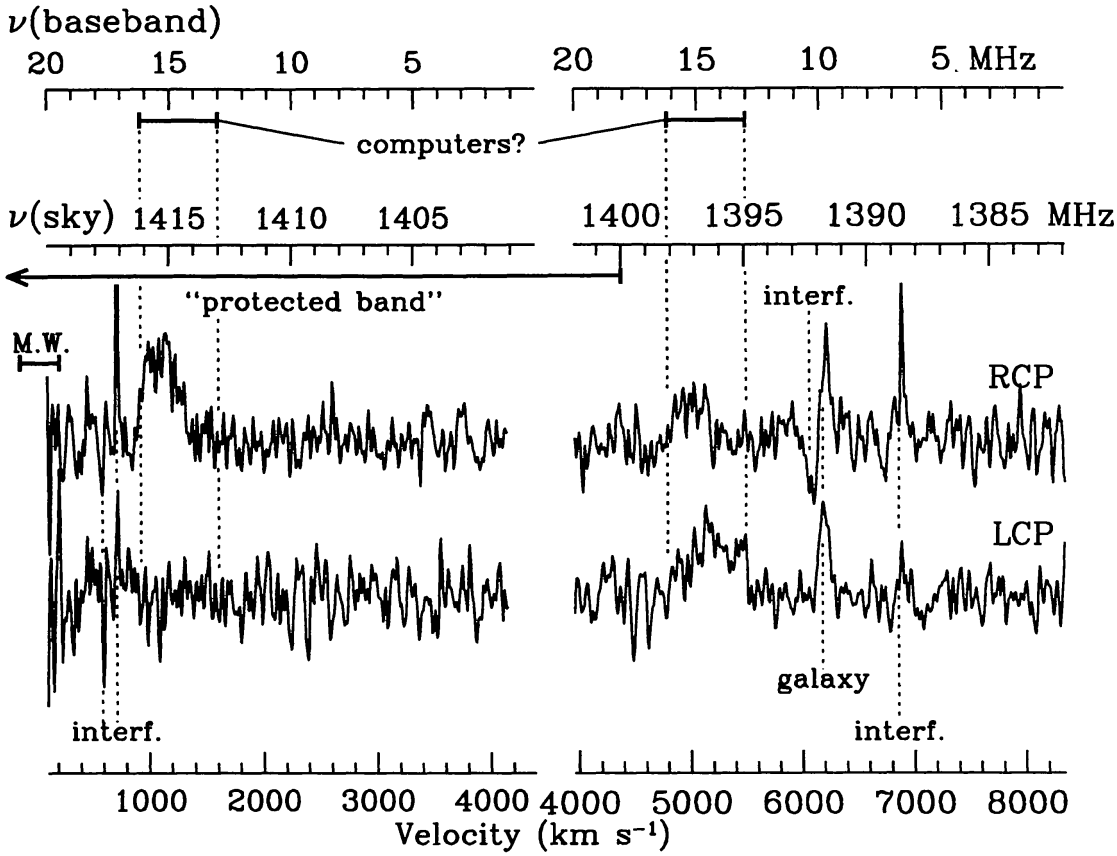

Figure 9. A 21-cm nightmare! A single observation made in two polarizations and in two segments of an autocorrelation spectrometer is shown to demonstrate how HI signals can be distinguished from interfering sources of emission.

emission is believed to be present. It is important to note that this baselining procedure can hide wide HI features or generate false signals when high-order polynomials are needed to match the spectrum's shape.

There are also small residual features where man-made interference and local Galactic emission have been imperfectly subtracted. Galactic emission makes searches for sources with redshifts smaller than a few hundred km s^{-1} difficult. Interference is not always easily identified, and it can enter at a variety of frequencies. As illustrated by the frequency scales at the top of Figure 8, the heterodyning procedures used in 21 cm observations allow interference to enter at several different frequencies besides the 21 cm range. It may be introduced in one or more intermediate frequency ranges (where most of the amplification is done) or in the baseband frequency range (where the autocorrelation spectrometer operates). This interference usually appears as a nearly self-subtracted feature swinging positive and negative within a narrow span of frequencies. This identifying sign-reversal reflects small changes in frequency between the times of the *on* and *off* scans or by a changing redshift Doppler correction in that time span.

Interference is sometimes less easily identified, as when it occurs only or mostly during the *on* scan. This can become very difficult to disentangle from real extragalactic emission. A 21 cm "nightmare" of interference is illustrated in Figure 9. This is one of the most confusing spectra I have encountered, but it illustrates how a real signal can be identified despite rampant interference. The spectrum shown is split up into the left and right circular polarizations that were simultaneously observed. Since HI emission is normally unpolarized, the polarizations are usually combined to improve the signal-to-noise. However, interfering sources are often highly polarized, so by studying the polarizations separately these sources can be identified. Since the system is relatively well-shielded at the intermediate frequencies, I suspect most of the interference entered at the sky frequency, even within the 21 cm "protected band" at frequencies higher than 1400 MHz.

There is also some broad interference that was probably introduced around 16 MHz in the baseband. This can be identified as baseband interference because two ranges of sky frequency were observed simultaneously (in order to span a wider range of redshifts). Since similar (though polarized) interference is seen at the same relative position in both of the right circularly polarized spectra, this signal is likely entering at a single baseband frequency. Given the frequency involved and the fact that a shielded door to the computer room was accidentally left open, it appears likely that this interference was generated within the observatory itself.

Even the galaxy detected in this spectrum is difficult to recognize because there is some interference overlapping it. However, it is the only signal with a consistent strength in both polarizations and without a parallel feature seen entering through the baseband in the other redshift range. This spectrum was so problematic that the observation was repeated (with the shielded door closed!), and the source was confirmed, but in principle the redundancy in the data allows one to identify sources despite widespread interference.

An implicit aspect of identifying these HI features in 21 cm spectra is the expected shape of the feature. In Figures 8 and 9 I've illustrated the two common classes of HI profiles, the so-called two-horn and one-horn profiles. Two-horned profiles are produced by rotating disks seen at an inclination larger than $\sim 20°$. The gas on opposite sides of the center is Doppler shifted to higher or lower frequencies than the systemic redshift of the galaxy, and combined with the flat rotation curves this results in strong emission at two frequencies. Single-horn profiles are produced by face-on disk galaxies, dwarfs, and irregulars, where random motions and/or the lack of a flat rotation curve generate a roughly Gaussian shape. See Skillman (chapter 8) for a more complete discussion.

In general, it is assumed that a 5-σ signal would be identified, where σ is based on the line-width of the signal. For example, a wide signal like that in Figure 8 has uncorrelated noise entering in each of the $N_{ch} = 45$ channels over which the signal is seen. Since each channel is $\Delta v = 8$ km s^{-1} wide, and has an rms uncertainty of $\sigma_{ch} = 4$ mJy, the total noise is:

$$Noise = \sqrt{N_{ch}} * \sigma_{ch} * \Delta v = 1.4\text{Jy km s}^{-1} \ . \qquad (6)$$

The signal is the sum of the fluxes detected in each channel. In this case average signal strength is $\bar{s}_{HI} = 46$ mJy above the continuum + baseline, so that the

total signal is:

$$Signal = N_{ch} * \overline{s}_{HI} * \Delta v = 16.6 \text{Jy km s}^{-1} \ . \qquad (7)$$

Thus a wide feature with the same mean flux density is in principle easier to detect than a narrow feature, although in objects with the same integrated signal the one that is narrower is easier to detect.

As with optical identifications, expectations about the shape of HI signals result in an additional selection effect that is difficult to quantify. Most observers will dismiss very narrow signals in a 21 cm spectrum if they are less than ~30 km s^{-1} wide, since such narrow lines are uncommon for galaxies but common for interference. On the other hand, wide profiles that do not have the expected steep sides may be assumed to be part of the baseline variations.

With these cautions in mind, we would like to survey the sky at 21 cm for HI sources in a way comparable to the great optical surveys. Given the integration times needed, and the point-by-point way in which 21 cm spectra are collected, observing the whole sky is impractical. Even a few square degrees require a significant amount of observing time, with little promise of any significant detections. As a result, large blind surveys have been made only rarely.

In some sense an enormous blind survey, consisting of all of the *off* scans ever collected, actually has been carried out already, but the data are not easily accessible. As discussed in the introduction to this chapter, a few objects have been discovered in *off* scans. However, the *off* scans tend to examine regions of the sky and redshifts that "shadow" the locations of cataloged galaxies, which introduces a potential bias into such a sample. Moreover, my impression is that the observers who have examined *off* scans for this purpose, myself included, have rarely devoted the sort of careful attention to possible weak signals in the *off* scan that they do to *on* scan positions where they expect to see a signal. After all, interference is so common that it hardly seems worth tracking down every small blip. Therefore the statistical results from these *off*-scan surveys are suspect.

A systematic blind survey has the advantage that interference can be monitored and persistent sources can be identified. Unlike a randomly placed *off* beam, a blind survey can map contiguous regions so that the survey is likely to get a "close hit" on a source as opposed to detecting it in the fringes of the beam. This sort of systematic mapping also allows for a much more efficient use of observing time, since the spectra can act as *off* scans for each other. By combining many scans into a single *off*, the noise introduced by the *off* scan can be almost entirely eliminated, resulting in an almost four-fold improvement over targeted *on–off* observations.

When observing a region of sky in a blind survey, the strategy is to maximize the effective search volume for the HI mass of the objects being sought. A fundamental choice that must be made in carrying out such a survey is illustrated in Figure 10: One can observe a large volume of space by either taking relatively few spectra of a distant region of space, or by making many more observations of a nearby volume of space.

It is not immediately obvious which is the more practical approach, although it can be shown that shallower surveys are generally more efficient. Consider a galaxy of a particular HI mass as illustrated in Figure 10. If that mass could be

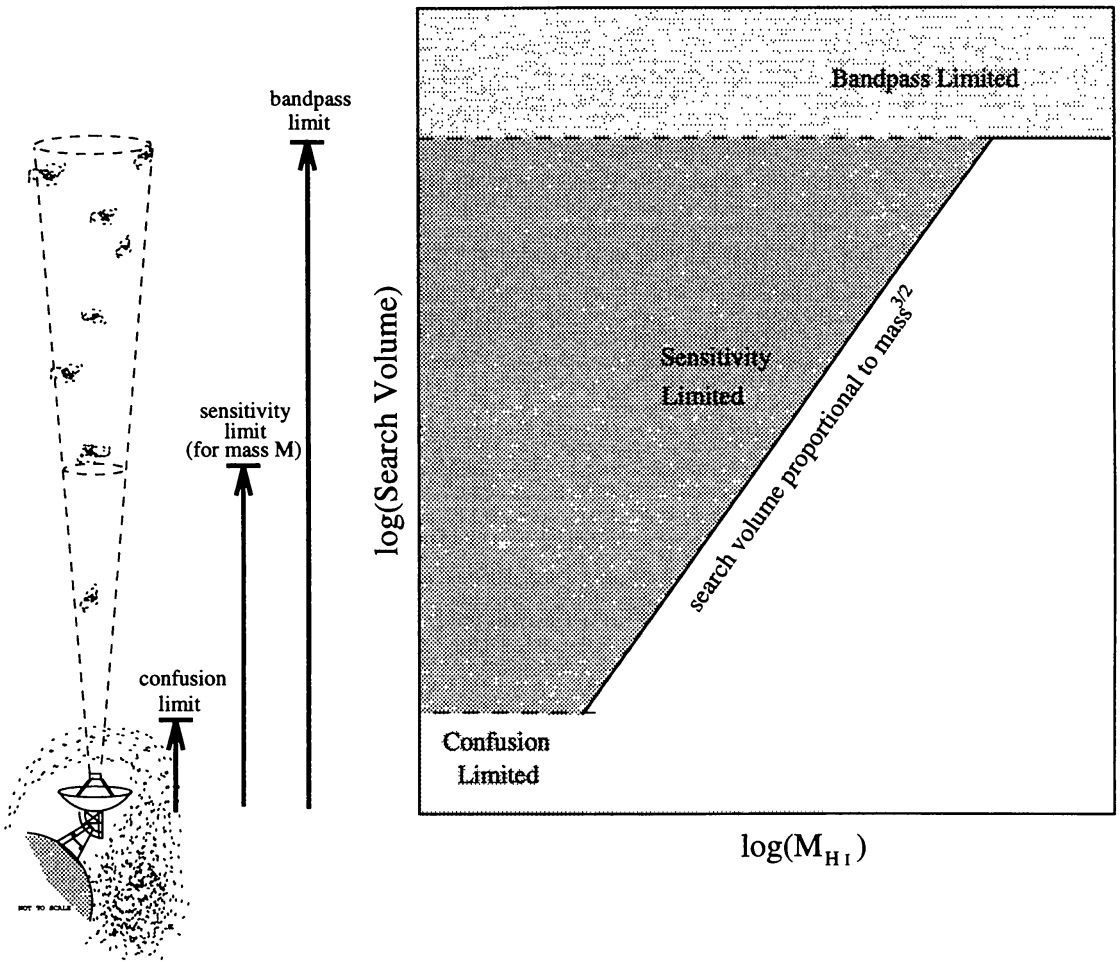

Figure 10. Schematic diagram of limits on search volumes in HI surveys. At small distances the search volume is affected by confusion with Galactic emission which can reach redshifts of several hundred km s^{-1}, which hinders a search out to many times the Galaxy's actual size. The effective volume being studied grows with mass until the bandpass limit of the survey is reached.

detected to twice the distance, we would expect to see $2^3 = 8$ times as many of these galaxies because of the increase in volume. However, at twice the distance, the signal is only 1/4 as strong, so the integration time to detect this mass is 16 times larger. Therefore it would take twice as long to survey the same volume of space as it would if we made 8 separate observations in different directions.

Taking this idea to its logical extreme the conclusion is that, given a fixed amount of observing time, it is optimal to observe as many positions as possible with the shortest possible integration time per position. This needs to be moderated slightly to recognize that *very* short integrations may not be useful (there aren't many galaxies within 1 kpc of us!), and the Doppler redshifts of HI in the Milky Way prevent us from detecting galaxies at redshifts smaller than $\sim$ 300 km s^{-1}. (Actually, massive galaxies can often be identified at low redshifts because of their distinct two-horn profile shape, but this is a minor point in terms of available search volume.) In addition, telescopic observations may become inefficient if integrations become so short that more time is spent moving the telescope than integrating on-source. A further limitation is that nearby galaxies usually have large angular diameters, so only a fraction of a galaxy will be detected within the telescope beam, and the integration times no longer improve at small distances. The ideal appears to be to integrate just long enough to detect the lowest-mass galaxies we are interested in several times further away than the distance at which their angular size matches the telescope beam size.

Having selected a survey strategy with a particular detection limit, the telescope detects the more massive galaxies out to higher redshifts. The detectable volume for these galaxies is larger in proportion to the cube of their detectable distance limit (equation 5) or $M_{HI}^{3/2}$. The bandwidth of the spectrum can introduce an upper limit on the volume for massive galaxies, and, depending on the set-up employed, there could be a limit at small redshifts as well.

The effective volumes surveyed in a number of the largest studies are shown in Figure 11. The effective volume for each survey is calculated from the velocity range and resolution, rms noise, beam size, and total number of points observed. The surveys by Krumm & Brosch (1984), Henning (1992), Shostak (1977), and Fisher & Tully (1981) were made at the Green Bank 300 ft telescope. The survey by Weinberg et al. (1991) was carried out at the VLA. The "Arecibo Slice" survey is a recent survey described later in this chapter.

One of the larger surveys illustrated in Figure 11 consists of *off* scans made in the course of studying cataloged galaxies as was discussed earlier. The "Off Scan" line represents an estimate of the volume covered in calibration scans by an assortment of Arecibo surveys primarily by myself and by Giovanelli & Haynes and collaborators. It is notable that only a few objects were picked up in these *off* scans, while Henning (1992) detected 37 objects in an almost identical search volume. Part of this difference is because these *off* scan surveys do not usually make note of previously cataloged galaxies that are accidentally detected, and they have also been quite unsuccessful at identifying low mass objects, probably because of the failure to distinguish narrow HI features from interference. It seems clear that despite their "serendipity potential," *off* scan surveys do not match the power of systematic surveys.

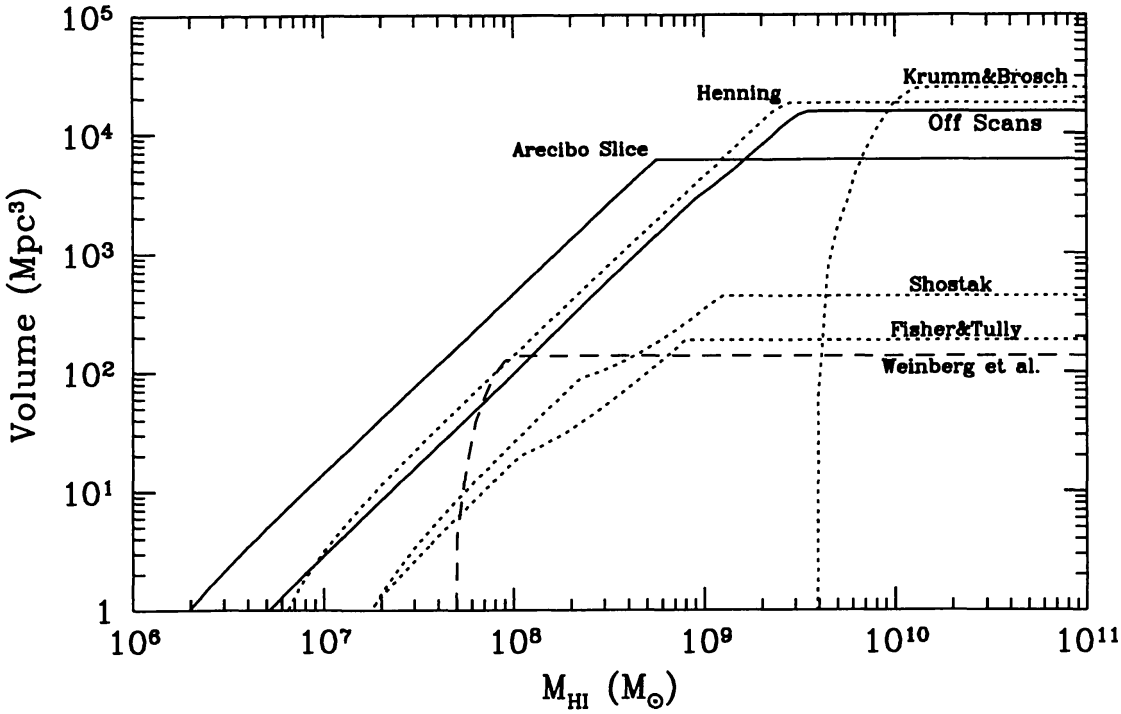

Figure 11. Volumes of space searched as a function of the detectable mass for a number of the largest HI surveys.

The diagram shows that the high mass end of the luminosity function has been probed fairly well, but the volumes studied at low masses are substantially smaller. The Henning survey is one of the best for a wide range of mass sensitivity, but unfortunately (for our purposes) it was mostly carried out at low Galactic latitudes where optical extinctions are large so that it is difficult to compare optical and 21 cm results. Another point not made by this graph is that the VLA survey by Weinberg et al. (1991) examines a realm of small angular sizes and separations that the other surveys are insensitive to because of confusion. Thus they are able to detect low mass companions to massive galaxies where the single dish surveys might simply assume the gas was part of the larger galaxy.

The recent surveys conducted by Henning (1992) and by Weinberg et al. (1991) do demonstrate the presence of a significant number of low mass HI sources. However, the relatively small number of new objects found by these surveys does not allow the HI luminosity function to be determined well for low masses. A deeper survey using the largest radio telescope available, the 305 m diameter Arecibo telescope, was the logical extension of their work. This survey is described in the next section, and its volume/mass function is illustrated in Figure 11.

6. The Arecibo Slice Survey

The new survey, which I undertook with my student John Spitzak, was made in a narrow "slice" at a declination of 23°, as illustrated by the gray region

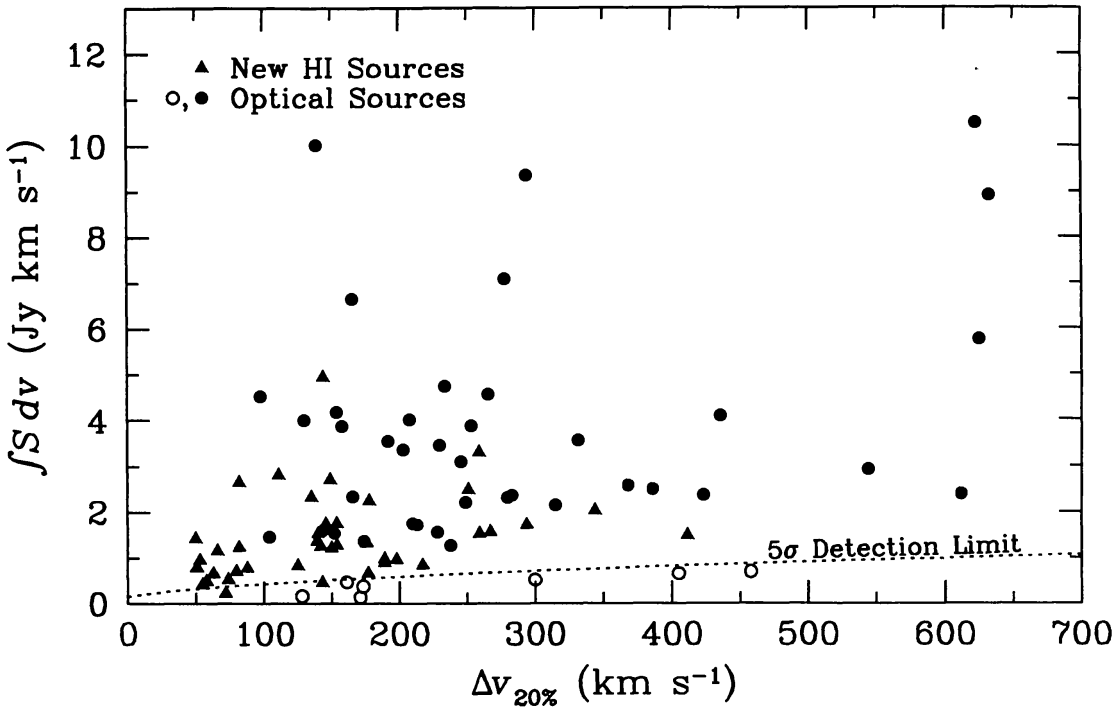

Figure 12. The integrated fluxes of sources detected in the Arecibo slice survey. Detected sources are shown with solid symbols, while undetected sources are shown with open symbols. A 5-σ signal-to-noise line, based on equations 6 and 7, appears to successfully describe the boundary of source detectability.

in Figure 6. The observations were made in a step–stare mode, keeping the telescope nearly pointing at the meridian while the sky rotated overhead. The region chosen is $> 30°$ from the Galactic plane so that optical extinction is small. This region in Pisces–Perseus was chosen because Giovanelli & Haynes (1988) had so thoroughly observed the cataloged galaxies that "proposal pressure" at the Arecibo telescope in this time range was relatively low. In consequence we were able to obtain over 300 hours of telescope time, with which over 14,000 spectra were obtained, covering about 50 square degrees.

Because the region had been so thoroughly studied in HI before our survey, we have a direct test of our success rate. We rediscovered every previously-detected galaxy that we should have given our sensitivity limit. We illustrate this point in Figure 12. The sensitivity limit derived from this figure and from our more general arguments about signal and noise contributions for HI signals of various widths also permits us to determine more precisely what the limiting volume is for each of our detections. We use this information later when we derive an HI luminosity function.

In summary, the slice survey detected 79 objects within its redshift search range of 400–8400 km s^{-1}. Half (38) of these were cataloged sources—found in one of the many optical catalogs contained in the NASA Extragalactic Database. The other half proved to be previously uncataloged objects, although almost all appear to have optical counterparts. This sample constitutes the largest

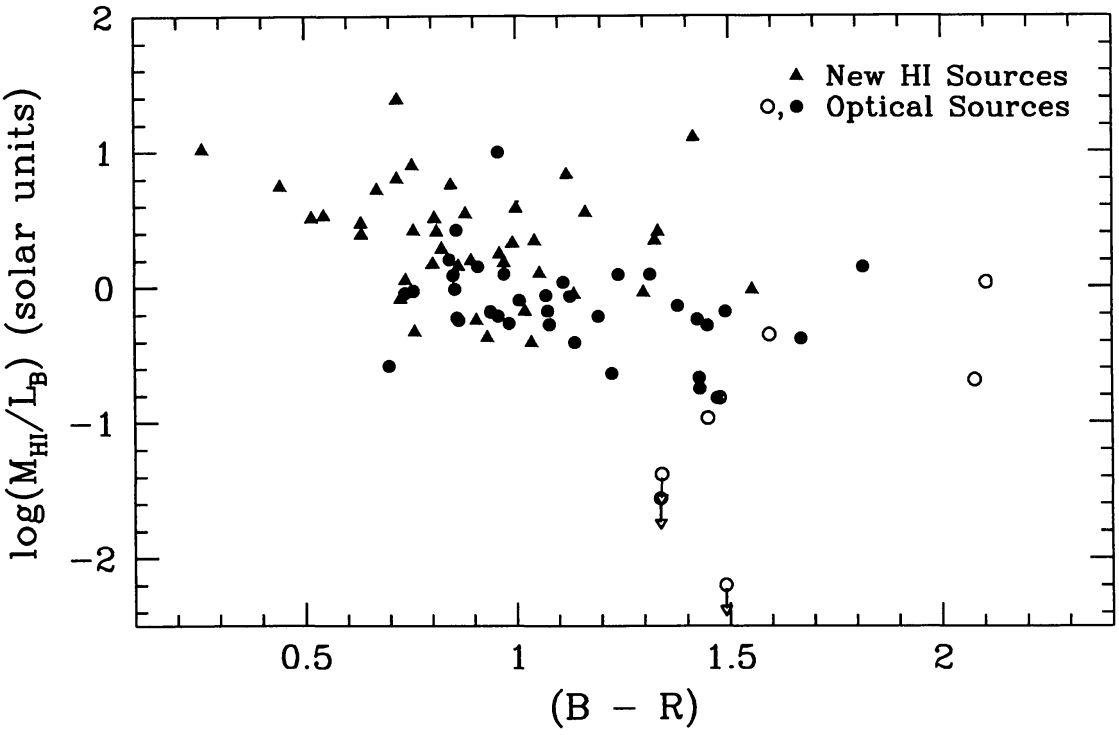

Figure 13. Comparison of HI-to-optical luminosity ratio to the mean optical color of galaxies in the Arecibo slice survey. The colors are extinction corrected integrated values out to the 25 mag arcsec^{-2} isophote in the blue.

collection of HI-selected objects yet found, and permits us to examine many of the questions raised in the earlier parts of this chapter.

The most fundamental question about these HI-selected objects is whether they represent a different population than the optically-selected sources or merely a deeper sample. For example, if optical and HI emission were exactly correlated, a deeper HI survey would pick up the same new sources as a deeper optical survey. If this were the case, the doubling in number of objects would imply an optical sample with a cutoff approximately 0.5 magnitude higher (i.e., a flux $2^{1/3}$ times fainter). However, while the previously cataloged objects have a sharp cutoff fainter than a blue magnitude of about $m_B = 15.5$, the new HI-selected sources have an average magnitude of $m_B = 17.5$ (6.3 times fainter), with some objects beyond 20th magnitude (100 times fainter).

Another way of illustrating the sample differences is presented in Figure 13. First note that the newly-found, uncataloged objects (solid triangles) have significantly higher levels of HI relative to their optical output—up to $\sim 10\times$ more solar masses of HI per solar luminosity of blue emission. The new objects also tend to be bluer than the previously cataloged optical sources, providing further evidence that these objects have different characteristics than an optically-selected sample. The blue colors of the new objects also demonstrate that the new objects should not have had any bias against their detection in optical surveys since most of these were conducted with photographic plates that are most sensitive in the blue.

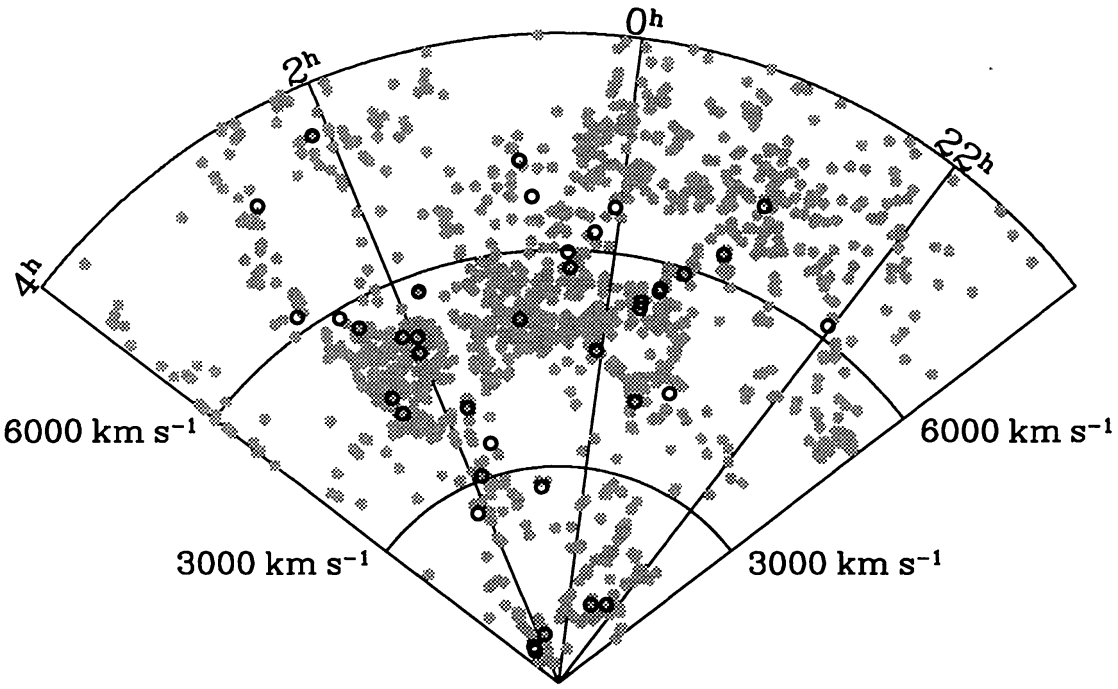

Figure 14. Locations of previously uncataloged galaxies found in the Arecibo slice survey. The actual survey limits were from about 22^h to 3^h, within the $23° < \delta < 24°$ declination band as shown in Figure 6. The black circles show the redshifts of the slice galaxies, while the positions of RC3 galaxies between $13° < \delta < 34°$ (but outside of the survey slice) are shown in gray.

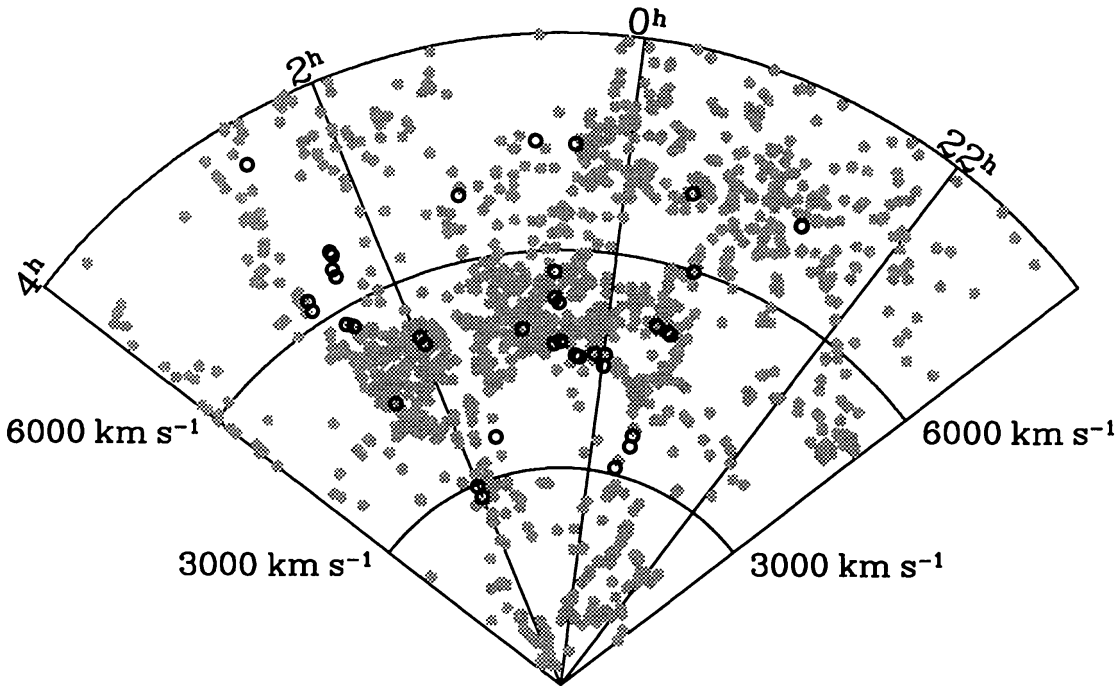

Figure 15. Locations of previously cataloged galaxies "rediscovered" in the Arecibo slice survey, as in Figure 14.

It appears from Figure 13 that there is a trend in the characteristics of these galaxies: blue galaxies have a larger proportion of HI. I would speculate that this might be an indication that the new-found objects have undergone less star formation and that a larger proportion of their mass remains in a reservoir of HI.

Another interesting question to examine is where these HI-selected sources lie relative to the large-scale structure defined by optically-selected sources. Dividing the sample into the cataloged and uncataloged parts, I illustrate the location of the objects in right ascension/redshift plots (often called slice diagrams) in Figures 15 and 14 respectively. For comparison, galaxies in the RC3 lying within $\pm 10°$ of the Arecibo slice (but excluding the slice area itself) are shown in gray. The large ridge of objects at ~ 5000 km s^{-1} is related to the Pisces-Perseus supercluster studied by Giovanelli & Haynes (1988).

More uncataloged objects are found in the slice at low redshifts, but both the cataloged and uncataloged objects tend to follow the same large-scale structure seen throughout the region. This suggests that the voids are not populated by HI sources, but it must also be recognized that the sensitivity to low-mass HI sources only allows them to be detected to relatively small distances. In any case, it does not appear that HI sources will redraw the boundaries of large-scale structure, although it appears that the census of even the "Local Supercluster" (at redshifts below ~ 2000 km s^{-1}) is incomplete.

7. A Gallery of HI-Selected Galaxies

The optical characteristics of the objects found in the Arecibo slice provide further clues about what makes a galaxy stand out in an optical survey. To explore these objects' characteristics, optical images obtained at the Kitt Peak 0.9 m telescope are shown in Figure 16. The 82 galaxies comprise 40 (of 41) uncataloged objects, 35 (of 38) cataloged objects, and 7 (of 10) optically identified galaxies within the slice volume for which R-band images were obtained. (This last category includes all but UGC 1538 among the cataloged objects in the first panel of Figure 16.) They are shown in order of increasing HI mass, with previously uncataloged objects running down the left of each panel and cataloged objects on the right.

Each image is displayed using the same logarithmic gray scale so that faint outer regions can be seen at the same time as the bright cores of some galaxies. The images are all scaled to the same linear size based on their Galactocentric velocities and assuming a Hubble constant of 75 km s^{-1} Mpc^{-1}.

Along the bottom of each image, the HI spectrum is shown with the same velocity scale in each case. The area under each of these HI profiles (i.e., the integrated flux) is again scaled logarithmically to the total HI mass of each object; this is to facilitate comparison without letting the range of sizes become unwieldy. Most of the HI profiles can be classified as single- or double-horned, although some are peculiar. The spectra are based on follow-up observations of the galaxies, in almost all cases after determining the centroid of the HI emission. As a result, most asymmetries in the profiles should not be caused by the placement of the object in the edge of the 21 cm beam. However, noise in

the spectra (particularly for the wide profile, distant objects) is sometimes large enough that it might generate artificial asymmetries.

The morphologies of the uncataloged vs. cataloged galaxies exhibit a variety of differences. Some of the uncataloged objects are so similar to their cataloged counterparts, that we might conclude they were accidentally overlooked, or that they fall in the category of being just slightly beyond the optical survey cutoff criteria. In general, though, the uncataloged objects have lower surface brightnesses, and are smaller on average than their optically-cataloged counterparts, so their omission from optical catalogs is not surprising. Some of the HI-selected objects are extremely low in surface brightness, with the lowest mass one (#90) having no identified counterpart.

The uncataloged objects show a weak trend of increasing size and brightness with their HI mass. In contrast, there does not appear to be any clear correlation of optical size or surface brightness with the HI mass of the cataloged objects; there are large and small galaxies at both extremes of HI mass. The HI linewidths, which are indicative of the total mass, do appear to correlate with both the increasing HI mass and optical size and brightness.

Morphologically, the HI-selected objects have a greater incidence of asymmetric light distributions and peculiar HI profile shapes. Almost all of the cataloged objects show a nearly stellar, very high surface brightness core, and a roughly elliptical outer boundary. The exceptions appear to be interacting galaxies, or low surface brightness galaxies uniquely identified by Nilson (1973) in the Uppsala General Catalog (UGC), whose aim was to make a size-limited catalog instead of a flux-limited catalog. The uncataloged objects only rarely have a bright central region, and sometimes the bright region is offset from the center.

For the most part, the optical-identification procedures *do* appear to have successfully identified the galaxies they were targeting. The additional galaxies identified in the HI survey almost all fall below the flux cutoff of the optical catalogs ($m_B > 16$) or have sizes smaller than the UGC's size limit ($a < 1'$). However, while the optical samples succeeded in identifying all of the most massive galaxies within the slice, they have overlooked a population of low surface brightness objects that in many cases appear to have equally large dynamical masses (based on their HI linewidths and estimated inclinations) as the galaxies of intermediate and low mass. We might expect then that the HI-selected sample will show a steeper luminosity (or mass) function than was found optically. We examine this next.

8. The HI Luminosity Function

The Arecibo HI survey provides us with all of the basic data we need to determine the HI luminosity function, and since HI mass and luminosity are normally proportional, we can phrase this directly in terms of HI masses. Assuming that we are dealing with a representative region of space, the ~6000 Mpc^3 volume surveyed overall should allow us to determine the typical number of objects of different HI masses. Unfortunately, the distance to which the survey is sensitive for low masses is much smaller (see Figure 11). At an HI mass of $10^7 M_\odot$, the survey only samples $\sim$ 15 Mpc^3 of nearby space, which is probably much less

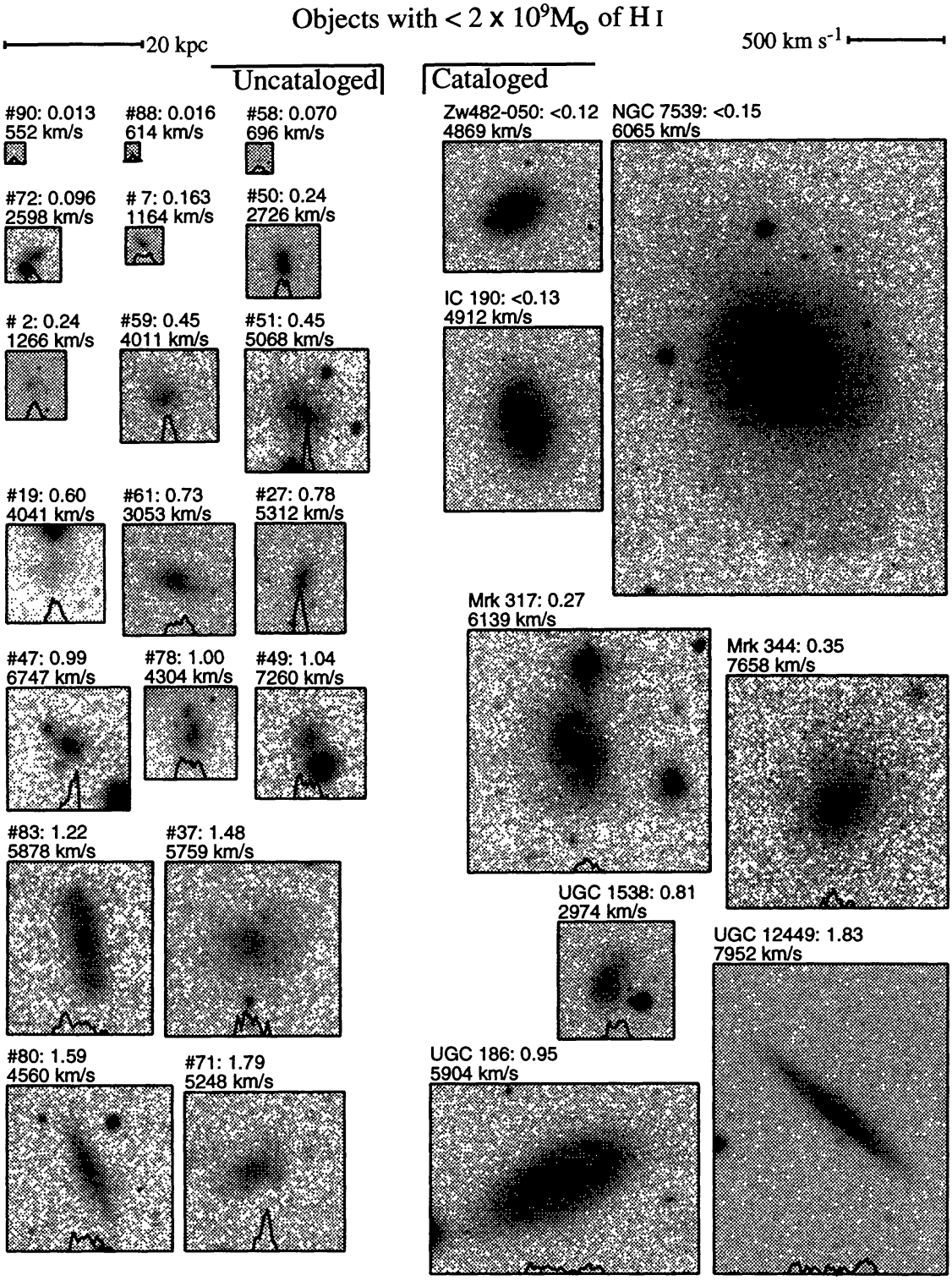

Figure 16. The Arecibo slice gallery. The images are all shown with the same logarithmic stretch on the same linear scale. The name or HI-catalog number is followed by the HI mass in units of $10^9 M_\odot$. The Galactocentric redshift is listed, and the HI profile is shown along the bottom of each image.

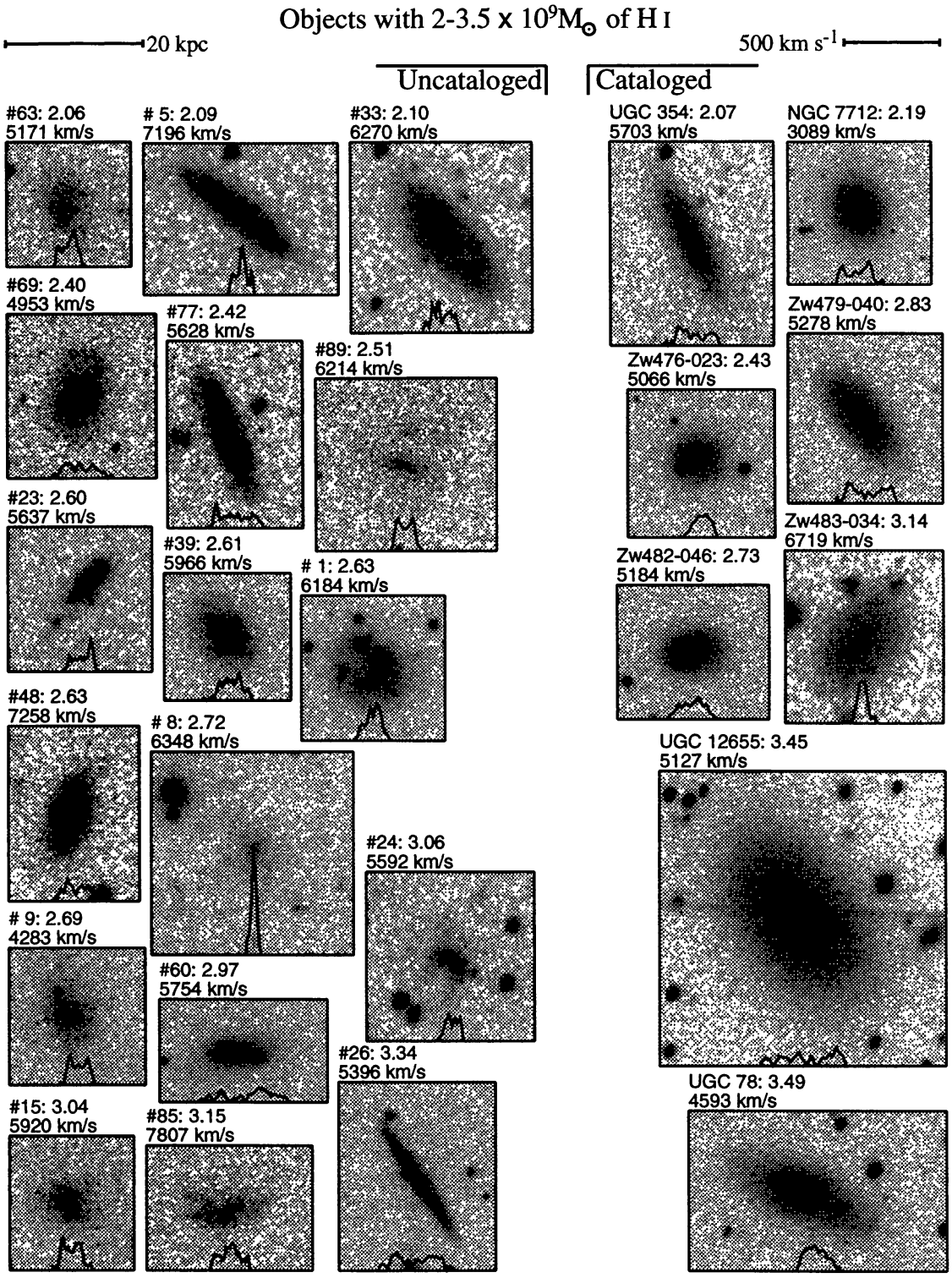

Figure 16. (continued)

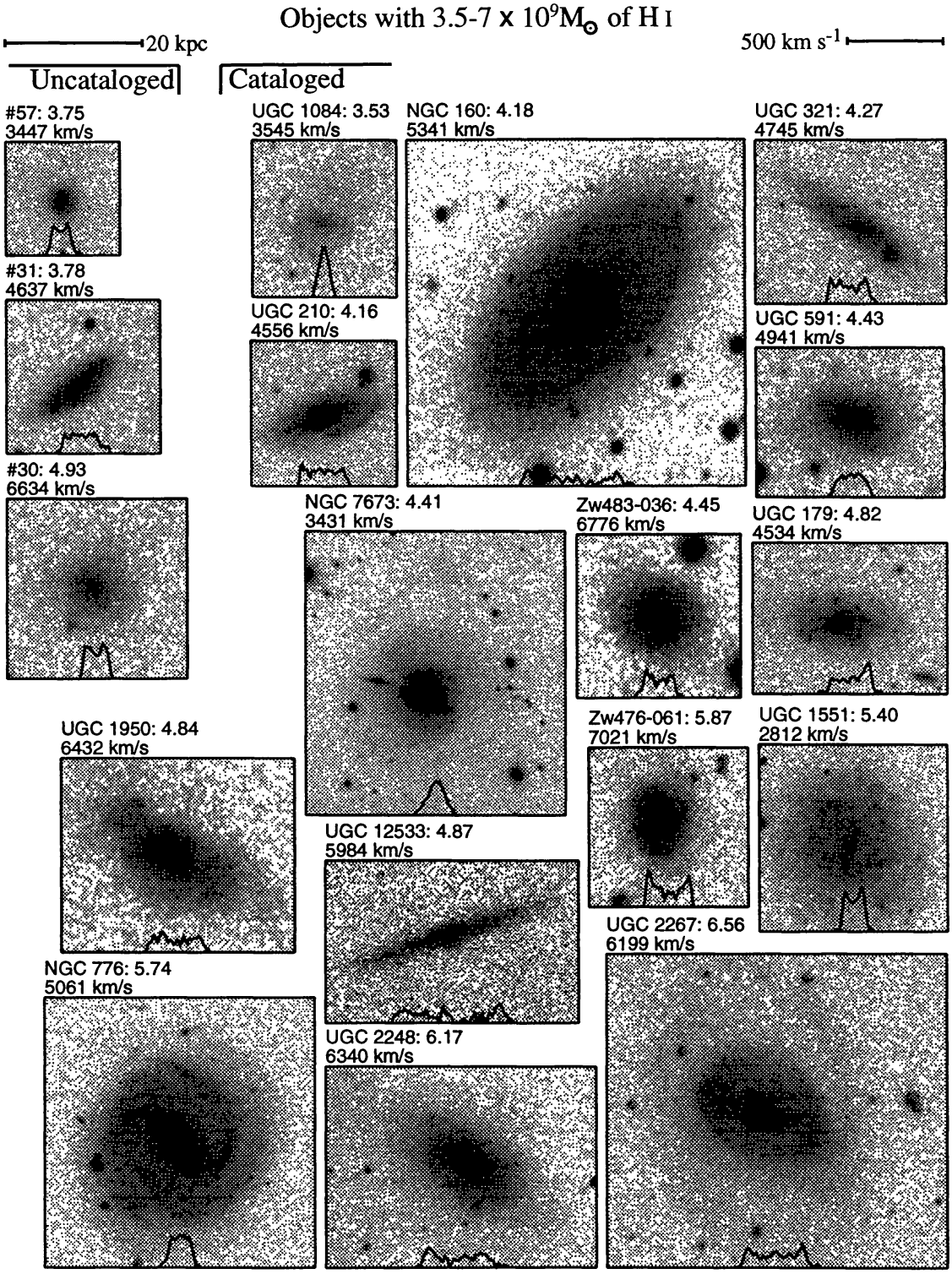

Figure 16. (continued)

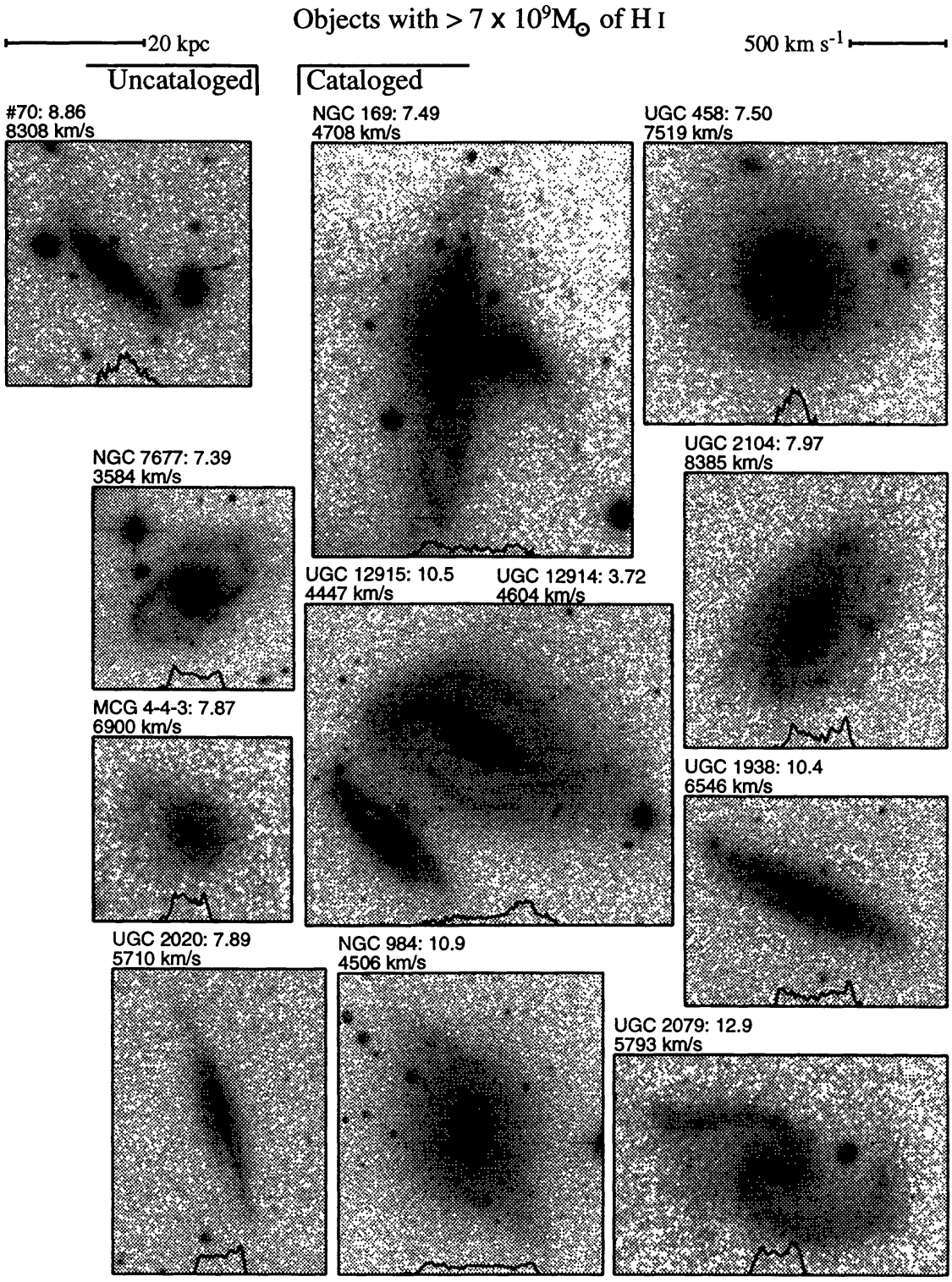

Figure 16. (continued)

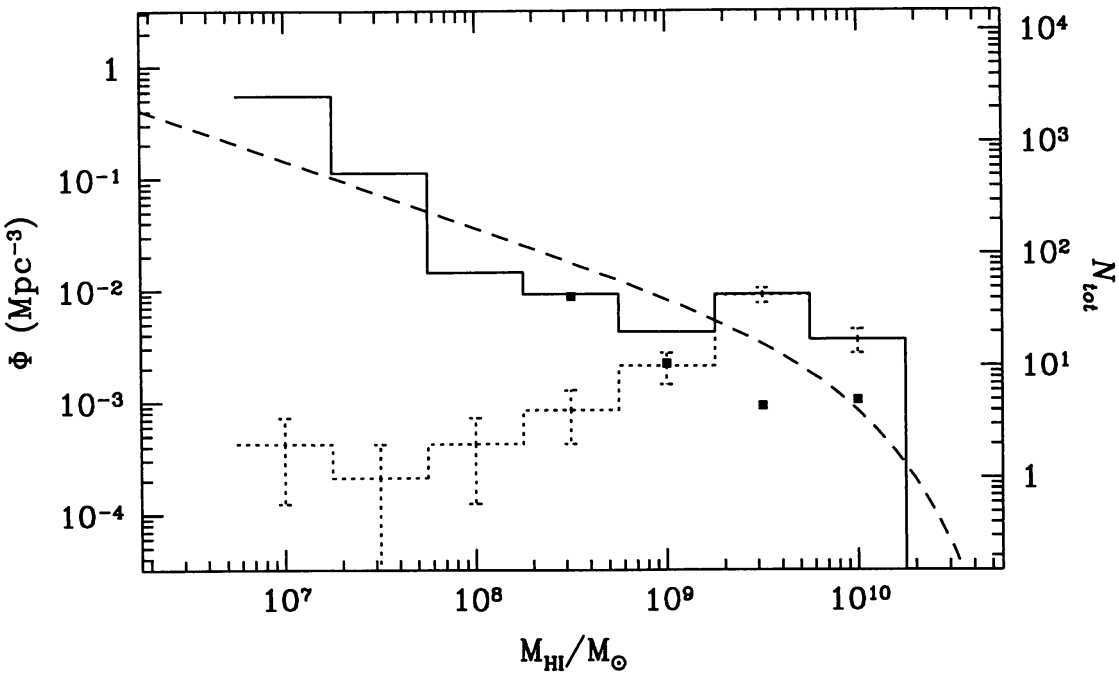

Figure 17. The HI mass function. The dotted-line histogram shows the number counts of galaxies actually detected in each half-decade logarithmic interval, with $N^{1/2}$ error bars. The solid histogram shows the sensitivity-corrected volume density of these same galaxies. Four squares show similar results from the HI survey of Henning (1995). The dashed curve is a Schechter luminosity function with $\alpha = -1.7$ and $M_{HI\star} = 10^{10} M_\odot$.

representative of the universe as a whole. Nevertheless, proceeding with fingers crossed, in Figure 17 I show the resulting density of galaxies in equal logarithmic intervals of HI mass.

Figure 17 shows the actual counts as a function of HI mass (dotted line) as well as the density of those sources (solid line) based on the limiting volume within which a source of that particular mass could be detected. Note how the number counts of detected sources drop to tiny numbers even as the number *density* grows to huge values. The Figure shows how $\sqrt{N}$ errors would affect the counts to give an idea of the uncertainty. The greater source of error is systematic: the resulting luminosity function depends critically on our estimate of how big a volume has been effectively surveyed for the low mass objects. To carry out this density estimate as accurately as possible, it is important to examine each source in more detail than just the average volume for that mass range. The method applied is to calculate the maximum distance (and hence volume) within which a similar signal could be detected accounting for its total HI mass, its HI linewidth, and the receiver sensitivity as a function of frequency.

The square symbols in the figure show the results from Henning's (1995) analysis of her Green Bank survey. The differences for massive galaxies suggest the range of uncertainty in sensitivity/volume estimates or possibly in variations across the sky. For the three lowest mass bins, the Arecibo survey was sensitive

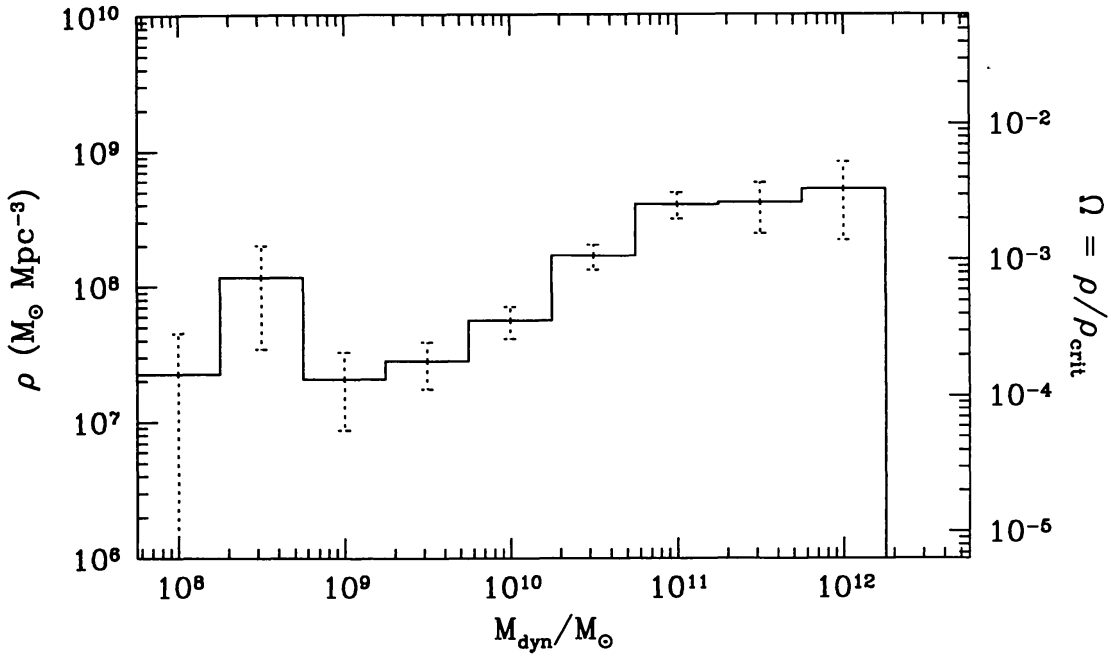

Figure 18. The mass function of galaxies projected from the HI-selected sample. Masses of each object were estimated from their size and rotation speed, and the total mass density contributed by galaxies in each logarithmic interval is calculated using the HI sensitivity corrections. $N^{1/2}$ error bars are based on the number of objects within each interval. The scale on the right gives the corresponding contribution of each mass interval to the closure density of the universe.

to several times more volume than the Green Bank survey, so it would not be expected that any galaxies would be detected in the Green Bank survey.

The dashed curve is a Schechter function with a power law index of $\alpha = -1.7$. It appears that HI is distributed among galaxies in such a way that there is a higher fraction of HI in small galaxies than the corresponding fraction of optical luminosity.

I close by returning to the basic issue raised at the beginning of this chapter. We are finally in a position to make a stab at the elusive mass function of galaxies. The path we've followed to reach this point has many potential pitfalls along the way, and the less adventurous may think it unwise to press forward. Nevertheless, with no small amount of trepidation, I offer Figure 18 for your perusal. This Figure shows the total mass density expected to be present in each mass interval based on dynamical mass estimates for each of the galaxies in the Arecibo survey.

Each galaxy's mass was estimated from its rotation speed (taken from the width of the HI profile) corrected for the inclination estimated from the the optical image. The Holmberg radius of each galaxy was then used to find its mass:

$$M_{dyn} = \frac{v^2 r}{G} \tag{8}$$

For the nine objects where the optical data were incomplete (and for the face-on objects whose rotation speed could not be estimated), we roughly estimated the total mass to be five times the HI mass, which is probably a conservative estimate. The same correction factors for sensitivity/volume were applied to each object according to its HI signal, and the mass densities in each interval were totaled to arrive at the mass function shown.

Since HI and total dynamical mass are not perfectly correlated, it is certain that this estimate is not going to be quite right, but the result suggests that galaxies make up at most about two percent of the closure density of the universe. The low mass galaxies, while not insignificant, do not appear to contribute as much as the high mass objects. The small number counts at the low mass end, however, leave this conclusion quite uncertain. Clearly, a deeper survey is needed, and I and others are currently in the process of examining new data collected at Arecibo while the telescope was partially crippled as it was being upgraded.

Looking toward the future, the total mass contributed by the galaxies found here is more than a factor of two lower than most estimates of the baryonic mass density determined from Big Bang deuterium synthesis. If, as some people believe, galaxies are mostly composed of non-baryonic matter, then only a fraction of the mass density found here is baryonic. It appears then that the story of where all of the primordial hydrogen went has not yet been told.

Acknowledgments. This work would not have been possible without the enormous effort of John Spitzak to complete the Arecibo survey. Portions of this project were supported by NSF Presidential Young Investigator award AST-9158096 and a UMass Faculty Research Grant. I would also like to thank the staff of the Arecibo Observatory for a great deal of assistance.

References

Binggeli, B., Sandage, A., & Tammann, G. A. 1988, ARA&A, 26, 509

Bothun, G. D., Impey, C. D., Malin, D. F., & Mould, J. R. 1987, AJ, 94, 23

Briggs, F. H. 1990, AJ, 100, 999

de Vaucouleurs, G., de Vaucouleurs, A., Corwin, H. G., Buta, R. J., Paturel, G., & Fouque, P. 1991 *Third Reference Catalogue of Bright Galaxies*, New York: Springer-Verlag

Deguchi, S., & Watson, W. D. 1985, ApJ, 290, 578

Disney, M., & Phillipps, S. 1983, MNRAS, 205, 1253

Dreyer, J. L. E. 1888, Mem. RAS, 49, Part 1

Fisher, J. R., & Tully, R. B. 1981, ApJ, 243, L23

Giovanelli, R. & Haynes, M. P. 1989, ApJ, 346, L5

Giovanelli, R. & Haynes, M. P. 1988, in Large-Scale Motions in the Universe, V. C. Rubin & G. V. Coyne, Princeton: Princeton University Press, 31

Henning, P. A. 1992, ApJS, 78, 365

Henning, P. A. 1995, ApJS, 450, 578

Krumm, N., & Brosch, N. 1984, AJ, 89, 1461

Kulkarni, S. R., & Heiles, C. 1988, *Galactic and Extragalactic Radio Astronomy*, eds. K. I. Kellermann & G. L. Verschuur, Berlin: Springer-Verlag, 95

McGaugh, S. S. 1996, MNRAS, 280, 337

McMahon, R. G., Irwin, M. J., Giovanelli, R., Haynes, M. P. & Wolfe, A. M. 1990, ApJ, 359, 302

Nilson, P. 1973, *Uppsala General Catalogue of Galaxies*, Uppsala Astr. Obs. Ann., 6

Puget, J. L. 1989, ARA&A, 27, 161

Schechter, P. 1976, ApJ, 203, 297

Schneider, S. E. 1989, ApJ, 343, 94

Schneider, S. E., Thuan, T. X., Magri, C., & Wadiak, J. E. 1990, ApJS, 72, 245

Schneider, S. E., Thuan, T. X., Mangum, J. G., & Miller, J. 1992, ApJS, 81, 5

Shostak, G. S. 1977, A&A, 54, 919

Stein, W. A. & Soifer, B. T. 1983, ARA&A, 21, 177

Telesco, C. M. 1988, ARA&A, 26, 343

Weinberg, D. H., Szomoru, A., Guhathakurta, P., & van Gorkom, J. H. 1991, ApJ, 372, L13

Zwicky, F., et al. 1961–1968, *Catalogue of Galaxies and Clusters of Galaxies*, Pasadena: California Institute of Technology